Chapter 13
Peptide and Protein Emulsifiers

Mohamed A. N. Soliman, Abdulwahhab Khedr, and Mohamed A. Elsawy

Abstract There has recently been a growing attention towards peptide and protein molecules as potential bioemulsifiers for the stabilization of foams and emulsions, thanks to their innate tendency towards interfacial adsorption. Additionally, peptides and proteins are biodegradable and biocompatible, making them less toxic if compared to traditional emulsifiers. This chapter provides a comprehensive overview of the different classes of peptide, protein and mixed protein–polysaccharide emulsifiers and discusses the emulsification mechanisms of these systems. In essence, peptide-mediated emulsification can occur either via traditional surfactant-like mechanism, where amphiphilic molecular peptide chains adsorb at the biphasic interface forming 'spherical micelles', or through peptide self-assembly into higher secondary structure (α-helices or β-sheets) with the formation of amphiphilic nanofibrous structures adsorbing at the interface. Moreover, peptides can self-assemble in the continuous aqueous phase forming nanofibrous network of viscous hydrogels that enhance system stability. On the other hand, emulsion stabilization by proteins is mainly achieved through either electrostatic repulsion or steric stabilization. The various characterization techniques for emulsification and interfacial stabilization will be visited throughout this chapter, focusing on structural, mesoscopic and macroscopic characterization of these systems.

M. A. N. Soliman
Leicester School of Pharmacy, Leicester Institute for Pharmaceutical Innovation, De Montfort University, Leicester, UK

Department of Pharmaceutics and Industrial Pharmacy, Faculty of Pharmacy, Cairo University, Cairo, Egypt

A. Khedr
Leicester School of Pharmacy, Leicester Institute for Pharmaceutical Innovation, De Montfort University, Leicester, UK

Department of Pharmaceutics and Industrial Pharmacy, Faculty of Pharmacy, Zagazig University, Zagazig, Egypt

M. A. Elsawy (✉)
Leicester School of Pharmacy, Leicester Institute for Pharmaceutical Innovation, De Montfort University, Leicester, UK
e-mail: mohamed.elsawy@dmu.ac.uk

M. A. Elsawy (ed.), *Peptide Bionanomaterials*,
https://doi.org/10.1007/978-3-031-29360-3_13

Keywords Emulsion · Emulgel · Emulsifier · Self-assembled peptide · Protein · Interfacial self-assembly

13.1 Introduction

Emulsifiers have been widely developed and exploited in many industries, such as wastewater treatment, improved oil recovery, food and beverages, detergents, cosmetics as well as coating industries, in addition to their utilization in chemical catalysis and cell assays (Moreira et al. 2017; Dexter et al. 2006; Lv et al. 2019; Dexter 2010; Bai et al. 2014; Platzman et al. 2013). Importantly, they have been used in various pharmaceutical formulations for drug encapsulation and controlled drug delivery (Dexter et al. 2006; Nishida et al. 2017; Windbergs et al. 2013; Naseef et al. 2018). Emulsifiers are required for controlling the characteristics of fluid–fluid interface, which is highly crucial for stabilization of foam and emulsion-based formulations (Dexter et al. 2006; Dexter 2010; Wilde 2000). Long-term stabilization remains as a pivotal challenge for these industries when developing such colloidal systems, which are instinctively thermodynamically unstable and vulnerable to phase separation (Li et al. 2016). Therefore, there is a crucial need for the development of emulsifiers that can enhance long-term stabilization while being biocompatible, non-toxic, sustainable and environment friendly (Li et al. 2016).

In essence, emulsifiers are a distinctive group of surfactants that can efficiently adsorb at different interfaces, particularly air–liquid and liquid–liquid, reducing interfacial tension and thus allowing for the dispersion of immiscible phases and formation of kinetically stable colloidal systems (Bouyer et al. 2012; Lee 2008; Mondal et al. 2017). According to Myers, emulsifiers can be classified into four main classes, based on their interfacial adsorption and emulsification mechanisms (Myers 1999). The first class includes non-surfactant ionic compounds capable of interfacial adsorption at drop surface resulting in electrostatic repulsions between close droplets, thereby stabilizing emulsions against coalescence. However, these ionic compounds neither impact the interfacial tension nor contribute to the emulsification steps. The second category comprises small non-surfactant colloidal solids, such as clay or silica, forming Pickering emulsions, as they adhere to droplet surface generating a physical barrier between globules that delays or prohibits coalescence. The third group encompasses the typical monomeric surfactant amphiphiles. They are composed of a charged/hydrophilic head conjugated to a hydrophobic tail. According to the inherent charge of the head part, they can be subdivided into anionic, cationic, zwitterionic or non-ionic molecules (Lee 2008; Caballero et al. 2003). At the interface, they adsorb and self-assemble, directing the hydrophilic head to the aqueous phase, whereas the hydrophobic tail towards the oil or gas phase forming protective layer preventing breakdown and lowering interfacial tension between phases, and consequently stabilizing the system (Petsev 2004). Finally, the fourth class contains polymer surfactants that impart steric and/or electrostatic stabilization to the system besides their interfacial tension diminishing capacity. They can also form cohesive interfacial films which inhibit the rupture of thin layers

of emulsifier surrounding the droplets or bubbles, which is the last stage in coalescence (Dexter et al. 2006; van Aken 2004). Moreover, they improve emulsion stability through enhancing elasticity and viscosity of the interface or by changing the bulk viscosity of the systems.

It can be noticed that interfacial adsorption and self-assembly is a common characteristic among the four classes of emulsifiers. Interfacial self-assembly is governed by mutual interactions between the emulsifier units and the interface itself. These interactions can also affect intermolecular forces between assembled emulsifier units and thus make the interfacial assembly significantly different from bulk self-assembly (Lee 2008). Better understanding of interfacial self-assembly processes can inform the rational design of emulsifier units that are capable of self-assembly at interfaces creating interfacial nanoarchitectures which can inhibit coalescence and coarsening (Scott et al. 2016).

Besides the molecular nature of emulsifiers, emulsions can be classified, according to the proportion and distribution of aqueous to oil phase in the system, into either simple or double emulsions. Simple emulsion may be either oil in water (O/W) when the oil is the dispersed phase and water constitutes the continuous phase or water in oil (W/O) which is the reverse state. Double emulsions are W/O/W or O/W/O systems offering merits over simple emulsions for encapsulation of therapeutic molecules and their controlled release due to the enveloped internal framework (Okochi and Nakano 2000; Hanson et al. 2008). The type of emulsion created, either O/W or W/O, depends on various intrinsic parameters including physicochemical properties of the emulsifier used, temperature and composition of the system. These parameters could affect the competition between coalescence tendency and emulsified droplet stabilization. In general, the highly stabilized phase will constitute the dispersed droplets, while the other phase coalesces forming the continuous phase (Lee 2008). Extrinsic manufacturing parameters can also affect emulsion order, such as the type of energy used (stirring), the way and time of its application as well as the order of ingredients mixing. Based on globular size and thermodynamic behaviour, emulsions can be classified into microemulsions (10–100 nm, thermodynamically stable), nanoemulsions (100–400 nm, kinetically stable) and macroemulsions (>400 nm, kinetically stable) (McClements 2012; Callender et al. 2017). The miniaturized size of nanoemulsions/microemulsions droplets shows several privileges over macroemulsions involving improved optical clarity, enhancement of drug cargo bioavailability and long-term formulation stability, which are all key attributes for drug delivery vehicle (Table 13.1) (Yang et al. 2017).

Although traditional emulsifiers are well suited for formation and stabilization of foams and emulsions, many of these emulsifiers are neither biodegradable nor biocompatible (Scott et al. 2016). Additionally, some have potential toxicity towards human health and the environment (Bouyer et al. 2012; Mondal et al. 2017; Rebello et al. 2014). Other limitations include impaired stabilization under environmental stresses, such as elevated temperatures, extreme pH ranges and high salt concentrations, as well as the insufficient long-term stability and not being amenable for structural modifications, all hindering their practical use in various industries

Table 13.1 Emulsion types and their properties

Emulsion	Type	Droplet size	Appearance	Energy input	Stability
Macroemulsion	Simple (O/W and W/O) and double (W/O/W and O/W/O) emulsions	>400 nm	Opaque turbid system	Required	Kinetic
Nanoemulsion		100–400 nm	Blue-white to semi-opaque system		
Microemulsion	Type I: Biphasic O/W Type II: Biphasic W/O Type III: Triphasic bicontinuous Type IV: Monophasic	10–100 nm	Single phase transparent system	Not required	Thermodynamic

(Adjonu et al. 2014; Fowler et al. 2011; Minkenberg et al. 2009; Lotfallah et al. 2015). Peptides and proteins came in the forefront as potential alternative emulsifiers that can overcome these limitations, thanks to the innate surface activity, biocompatibility and physicochemical tunability.

In this chapter, we will shed the light on recent advances in formulation of emulsions and foams using peptide, protein and mixed protein/polysaccharide emulsifiers. The various mechanisms of emulsification and interfacial stabilization will be discussed in terms of their structural and mesoscopic characteristics and their stabilization efficiency for longer term and under drastic conditions.

13.2 Peptide Emulsifiers

Peptide molecules possess the inherent characteristics of proteins, such as the biodegradability, biocompatibility and safety with additional advantages of low production costs with high purity and low batch-to-batch variations (Moreira et al. 2017; Li et al. 2016; Wibowo et al. 2017). In addition, exploitation of the amino acid chemical toolbox provides infinite possibilities of various chemical designs, enabling physicochemical tunability of peptide emulsifiers, for instance, tailoring hydrophilic and lipophilic properties and controlling the non-covalent electrostatic or hydrophobic interactions between molecules, which are essential for controlling interfacial self-assembly (Wibowo et al. 2017). Peptides can rapidly adsorb to interfaces at lower concentrations compared to proteins, facilitating droplet or bubble formation which is the most critical step for emulsion or foam formation, respectively. This is normally followed by interfacial adsorption into rigid cohesive

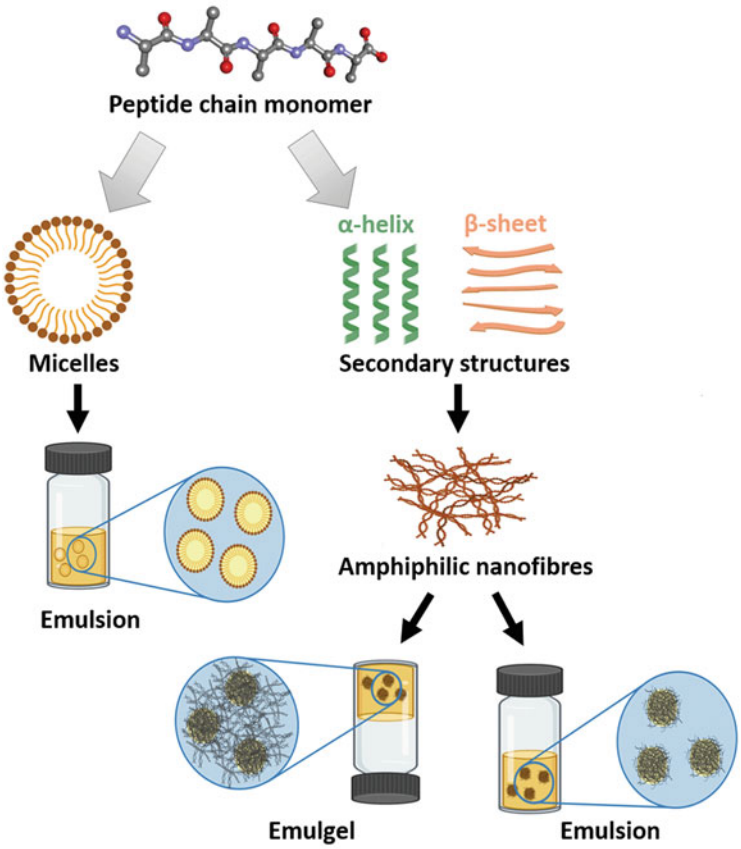

Fig. 13.1 The possible mechanisms of interfacial arrangement of peptide emulsifiers at the droplet interface through either micelle formation or self-assembly into nanofibrous structures, forming emulsions or emulgels

structures surrounding the droplets or bubbles maintaining their attachment and stabilization of these system (Scott et al. 2016).

Interfacial adsorption of peptide molecules can lead to the formation of micellar structures, akin to conventional surfactant, where the hydrophilic heads are solubilized in aqueous phase and the hydrophobic tail projecting to the organic or gas phase (Fig. 13.1). Interfacial self-assembly into higher secondary structure (α-helices or β-sheets) could also happen, forming amphiphilic nanofibrous structure at the interface (Fig. 13.1). Additionally, self-assembly into nanofibrous network in the bulk aqueous phase could occur, leading to hydrogel formation, which increases the system's viscosity and hinders emulsion coalescence or foam collapse, a system known as 'emulgel' (Fig. 13.1).

Based on their chemical structures, peptide emulsifiers can be classified into short aromatic, α-helix, β-sheet and surfactant-like peptides. In this section we will present

these different classes and will discuss their interfacial adsorption mechanisms in more details.

13.2.1 Short Aromatic Peptide Emulsifiers

Short synthetic peptides were developed to self-assemble into a variety of higher nanostructures, as discussed in Chap. 4: short peptide and peptidomimetic nanomaterials. Interestingly, short aromatic peptides have been designed to self-assemble into amphiphilic nanofibrous structures which exhibit interfacial activity. For instance, the Ulijn group reported the ability of amphiphilic dipeptides, which are N-capped with aromatic moieties, to self-assemble into nanofibrous networks at organic/aqueous interfaces (Fig. 13.2a) (Bai et al. 2014). Unlike traditional emulsifiers, which work via adsorption of the molecular amphiphile at the biphasic interface forming micellar structures, these short aromatic peptides form interfacial nanofibrous stabilization matrices (Figs. 13.1 and 13.2a). The 9-fluorenylmethoxycarbonyl tyrosine-leucine (Fmoc-YL) is one example of these short aromatic peptide emulsifiers, which was successfully used to stabilize chloroform-in-water emulsion by hand shaking for few seconds at 80 °C (Table 13.2). Interfacial self-assembly of Fmoc-YL into a less ordered β-sheet-like assemblies occurred via interchain hydrogen bonding (H-bonding) between peptide backbone amides as well as aromatic π stacking of Fmoc capping groups, forming amphiphilic nanofibrous structures, which entangle into interfacial network film stabilizing the suspended chloroform droplets within the aqueous continuous phase (Figs. 13.1, 13.2a, g and i). The Fmoc-YL-based emulsion exhibited greater stability (months) at room temperature than the commercial emulsifier sodium dodecyl sulphate (SDS), with the latter showing phase separation within 2 weeks. In addition, better thermal stability as well as resistance to salting out were achieved with Fmoc-YL in comparison to SDS emulsifier.

On-demand demulsification of Fmoc-YL systems was made possible using thermolysin protease enzyme, which digested the interfacial peptidic film under mild physiological conditions. Fmoc-YL also showed to be a successful emulsifier for other organic phases, such as hexadecane and mineral oil. Replacement of L residue in Fmoc-YL with A or S also produced peptide emulsifiers that formed chloroform-in-water emulsions. However, these changes significantly affected the emulsion characteristics, such as globular size and critical emulsion concentration. In case of Fmoc-YA, reduction of sequence hydrophobicity arising from replacing L by A did not influence β-sheet nanofibres formation in water. However, introduction of S impaired the peptide tendency to self-assemble into nanofibrous structures; consequently, higher critical emulsion concentration and emulsion globular size were observed for Fmoc-YS compared to both Fmoc-YL and Fmoc-YA (Table 13.2 and Fig. 13.2a–c). In essence, increasing both hydrophobicity and H-bonding interactions enhanced interfacial adsorption and lowered the emulsion droplet sizes as well as critical emulsion concentrations. To increase sequence

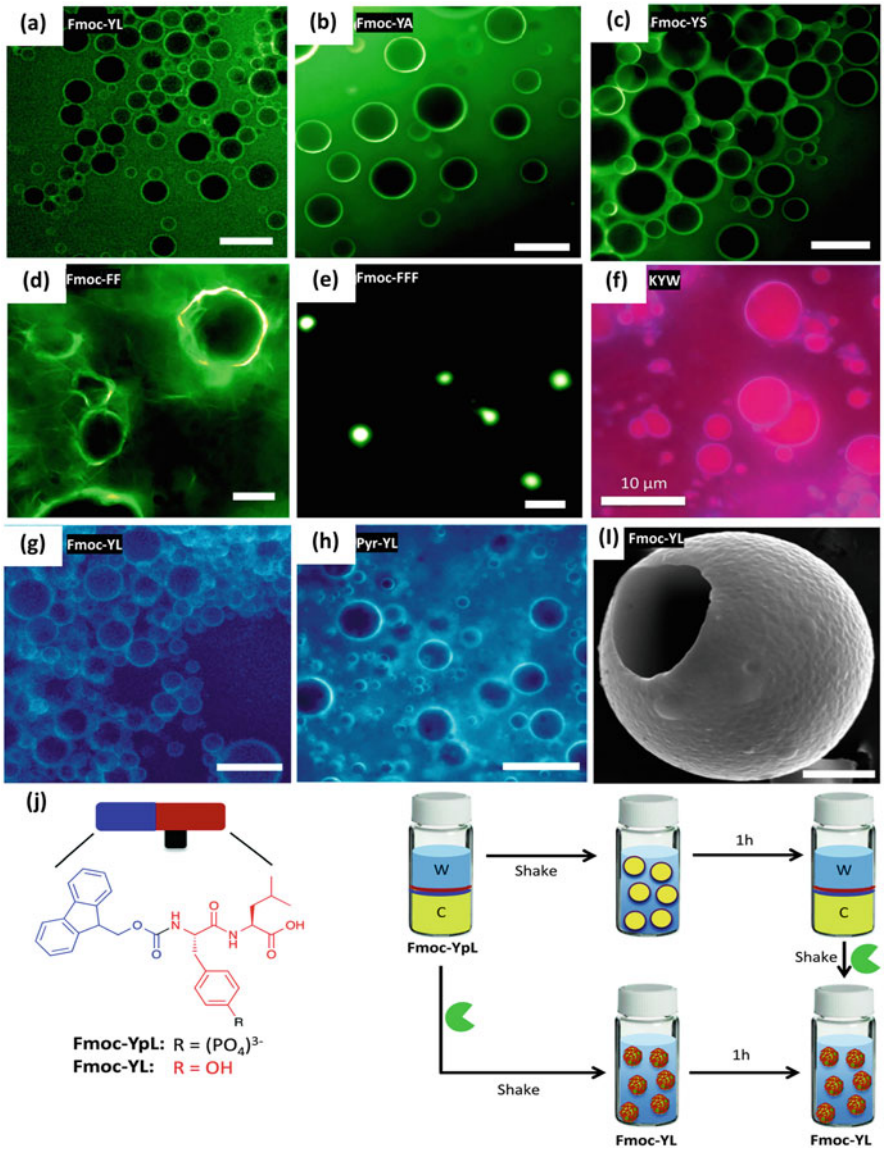

Fig. 13.2 Fluorescent microscope images of chloroform-in-water emulsion droplets stabilized by (**a**) Fmoc-YL, (**b**) Fmoc-YA, (**c**) Fmoc-YS, (**d**) Fmoc-FF networks containing fluorescence isothiocyanate (FITC) in water phase, (**e**) water-in-chloroform emulsion droplets stabilized by Fmoc-FFF containing FITC in water phase and (**f**) Fluorescence microscopy of KYW chloroform-in-water emulsion droplets with overlay of Sudan II and Thioflavin T (ThT) staining, (**g**) Fmoc-YL and (**h**) Pyrene-YL emulsions. Scale bar is 50 µm except for KYW (10 µm). (**i**) SEM micrograph of air-dried Fmoc-YL microcapsules at chloroform/water interface. Scale bar is 2 µm. Adapted from (Bai et al. 2014), with copyrights permission from the American Chemical Society and (Scott et al. 2016), with copyrights permission from John Wiley and Sons. (**j**) left. Chemical structure of Fmoc-YpL and Fmoc-YL, Right, Schematic representation of the Fmoc-YpL before and after alkaline phosphatase dephosphorylation in a biphasic system, showing Fmoc-YL stabilized emulsions,

lipophilicity, Fmoc was replaced by pyrene or YL by FF, where the Fmoc-FF and Pyr-YL successfully created chloroform-in-water emulsions (Fig. 13.2d, h). Further increase in lipophilicity resulted in inverted emulsion (water-in-chloroform), when using the highly hydrophobic tripeptide Fmoc-FFF as emulsifier (Fig. 13.2e and Table 13.2).

Ulijn and co-workers have also introduced biocatalytic-controlled interfacial self-assembly of phosphorylated Fmoc-YL (Fmoc-YpL) at chloroform/water interface using a phosphatase enzyme (Fig. 13.2j and Table 13.2) (Moreira et al. 2016), inspired by Xu's group strategy who first demonstrated that enzymatic dephosphorylation of Fmoc-tyrosine phosphate (Fmoc-Yp), using alkaline phosphatase, triggered self-assembly of the product Fmoc-Y into supramolecular hydrogel (Yang et al. 2004). Ulijn and co-workers demonstrated that the parallel arrangement of fluorenyl groups of Fmoc-YpL led to the formation of micelles, which when dephosphorylated by alkaline phosphatase into Fmoc-YL rearranged into fibrous structures at the organic/aqueous interface (Fig. 13.2j). The phosphorylated precursor Fmoc-YpL behaved as an amphiphile with surfactant-like adsorption, where the hydrophobic Fmoc tail projected to organic phase while the hydrophilic YpL chain head to water with low emulsion stabilization, with phase separation occurring within 1 h. Upon enzymatic dephosphorylation into Fmoc-YL, interfacial self-assembly into nanofibrous network was achieved via non-covalent interactions, as explained above, forming a very stable emulsion with no phase separation observed for months. The same group showed the possible conversion of a phase separated biphasic oil/water mixture containing Fmoc-YpL stored for up to 1 month into emulsion catalysed by enzymatic dephosphorylation. However, slower emulsification rate was observed compared to the immediate activation approach, with the formed emulsion exhibiting less stability and larger droplet size. This is attributed to the slower dephosphorylation of Fmoc-YpL leading to less ordered H-bonding, hence impairing the interfacial self-assembled fibrous network. Molecular dynamic simulation suggested the absence of permanent H-bonding between Fmoc-YpL monomers, while the dephosphorylated form showed Fmoc/L and Y/L H-bonding that agreed with FTIR results. Results of this study confirmed the importance of interfacial self-assembly of nanofibres for emulsion stabilization rather than individual peptide monomers (Fig. 13.1) (Moreira et al. 2016).

Although the Fmoc-capped dipeptides exhibit good surface activity, which was shown to be better than commercial emulsifiers in many cases, its potential translation to emulsifiers in food, pharmaceutical and cosmetic industries was withheld as the molecular design is based on the non-biological Fmoc group, which could potentially impair the biocompatibility of these materials. To overcome this limitation, Ulijn and co-workers developed unprotected tripeptide emulsifiers, with a peptide sequence design of two successive aromatic residues (Ar) flanked with a

Fig. 13.2 (continued) while Fmoc-YpL acted like a conventional surfactant and system separated into two phases after 1 h. Adapted from (Moreira et al. 2016), with copyrights permission from Royal Society of Chemistry

Table 13.2 Classes of peptide emulsifiers and their application

Class of emulsifier	Sequence of peptide	Emulsion/Foam type	References
Short aromatic peptides	Fmoc-YL	Chloroform-in-water emulsion Hexadecane-in-water emulsion Mineral oil-in-water emulsion	Bai et al. (2014)
	Fmoc-YA, Fmoc-YS, Pyr-YL, Fmoc-FF	Chloroform-in-water emulsion	
	Fmoc-FFF	Water-in-chloroform emulsion	
	Dephosphorylated Fmoc-YpL	Chloroform-in-water emulsion	Moreira et al. (2016)
	FFD, DFF, KFF, KYW, KYF	Rapeseed oil-in-water emulsion and oleic acid-in-water emulsion	Scott et al. (2016), Dragulska et al. (2018)
	Dephosphorylated KYpF	O/W emulgel	Moreira et al. (2017)
	Fc-FFD, Fc-FFH, Fc-FFS, Fc-FFF	Ethyl acetate-in-water emulsion	Yang et al. (2017)
	Nap-FF, BrNapFF, 2Nap-FF	Wet foams Isopropyl myristate, dodecane and silicon oil-in-water emulsions	Li et al. (2016), Aviño et al. (2017), Li et al. (2014)
Alpha helices forming peptides	SHR-FLLF, SHR-FLELF, SHR-FLKLF	Silicon oil-in-water emulsion	Mondal et al. (2017)
	AM1	Foam Toluene-in-water emulsion	Dexter et al. (2006) Dexter and Middelberg (2007), Middelberg et al. (2008)
	Lac21E	Foam	Middelberg et al. (2008)
	AFD4	Foam	Dexter and Middelberg (2007)
	AM-S	Foam	Wibowo et al. (2017)
	C8-AM	Miglyol 812 oil-in-water nanoemulsion	Wang et al. (2017)
	SurSi	Miglyol 812 oil-in-water nanoemulsion and silica nanocapsules	Wibowo et al. (2014), Hui et al. (2016)
	DAMP1, DAMP4 and their mixture	Foam	Middelberg and Dimitrijev-Dwyer (2011), Dwyer et al. (2013)
	SP16	Foam	Zhao et al. (2017)
	PBLG ($n = 12$ and 32)	Dichloromethane-in-water microemulsion	Morikawa et al. (2005)

(continued)

Table 13.2 (continued)

Class of emulsifier	Sequence of peptide	Emulsion/Foam type	References
		Dichloromethane/methanol-in-water microemulsion	
	$K_x(rac\text{-}L)_y$, $R_{40}(rac\text{-}L)_{10}$, $E_{40}(rac\text{-}L)_{10}$, $K_{60}(rac\text{-}V)_{20}$, $K_{60}(rac\text{-}A)_{20}$	W/O/W emulsion	Hanson et al. (2008)
	$K_{60}L_{20}$	O/W emulsion	Hanson et al. (2008)
β-Sheets forming peptides	B-14, B-15, B-16, B-17	Dodecane-in-water emulsion	Dexter (2010)
	Q11	W/O emulsion	Tian et al. (2011)
	A_9R	O/W emulsion	Castelletto et al. (2019)
	Phg4	Chloroform-in-water emulsion Melissa oil-in-water emulgel	Wychowaniec et al. (2020)
Miscellaneous peptides	GAP	Isopropyl myristate oil-in-water emulsion	Lotfallah et al. (2015)
	C_{13}-KR	Medium chain triglyceride oil-in-water emulsion	Lv et al. (2019)
	NH_2-lauroylGGGH/1,4-phthalaldehyde mixture	O/W emulsion	Nishida et al. (2017)

charged residue ($X^{+/-}$) either from the N- or C-terminus (i.e. $X^{+/-}$-Ar-Ar or Ar-Ar-$X^{+/-}$) (Scott et al. 2016). Two types of tripeptide emulsifiers were developed, the anionic (such as FFD and DFF), which formed bilayer-like assemblies at the oil/water interface, and the cationic (such as KFF, KYW and KYF), which formed interfacial nanofibrous networks that highly stabilized the rapeseed oil-based emulsions compared to the anionic type (Table 13.2). Interestingly, the cationic tripeptides self-assembled in both aqueous and biphasic media through H-bonding into β-stranded fibres, while the anionic tripeptides only showed interfacial self-assembly upon introduction of oil to the aqueous phase, where peptide chains stack into parallel orientation at the oil/water interface with lateral H-bonding interactions. The nanofibre forming peptide emulsifier KYF possessed superior thermal stability with no phase separation observed for the formed O/W emulsion at 80 °C, while KYW and KFF showed thermal stability only up to 50 °C and 40 °C, respectively, due to the breakdown of fibrous structure. Based on this, KYF was exploited as an emulsifier to formulate O/W nanoemulsion that can entrap oleic acid-platinum II conjugate for treatment of ovarian cancer (Dragulska et al. 2018). A nanoprecipitation method was employed by a dropwise addition of organic phase (oleic acid-platinum II conjugate in isopropanol) to aqueous phase (KYF dissolved in water at 37 °C and pH 7) with stirring overnight to prepare the nanoemulsion. The

miniaturized droplet size (240 nm) enabled its ability for extravasation and passive targeting of tumours with long-term stability upon storage for months. This strategy can be employed to encapsulate and deliver other active moieties.

Besides nanoemulsion formation, Moreira et al. demonstrated the ability of the phosphorylated tripeptide analogue KYpF to act as on-demand emulsifier that stabilizes O/W emulsion and emulgel upon treatment with alkaline phosphatase (Table 13.2) (Moreira et al. 2017). Complete dephosphorylation occurred 24 hours after incubation with phosphatase enabling the transformation of a biphasic system containing few micelles of KYpF at the interface (40 mM) into an O/W emulsion at low enzyme concentration and O/W emulgel at high enzyme concentration where both were stabilized by the dephosphorylated KYF. Emulsion stabilization was achieved via creation of β-sheet nanostructures at the oil droplet surfaces lowering interfacial tension, while emulgel additionally has crosslinked β-sheet nanofibres in the aqueous phase that enhanced the continuous phase viscosity. Enzyme concentration was found to be a crucial factor in controlling the emulsifying capacity of the peptide, as it affects the rate of self-assembly and densities of fibrous networks at the interface hindering coalescence. Increasing enzyme concentration led to faster dephosphorylation, higher levels of π–π stacking, more organized H-bonding between backbone amide of peptide chains, and overall better self-assembly and control of emulgel properties. The lowest enzyme concentration tested (0.07 μM) did not form emulgel but stabilized the emulsion through short un-entangled thick fibres (14 nm width), while increased entanglement and dense thin fibres (3 nm) appeared with the highest concentration (6.6 μM), stabilizing the system for more than 1 week. On the other hand, there was no evidence of secondary structure formation of KYpF in the absence of enzyme. The failure of KYpF assembly was ascribed to the hydration of phosphate ions in water rather than the repulsion between the anionic groups, so modifying the peptide hydrophilicity can affect self-assembly. The best catalyst concentration of the enzyme was 3.3 μM that produced sharper peaks at 1620 and 1560 cm^{-1} in FTIR. Interestingly, the biocatalytic emulsion formation was thermo-reversible displaying switchability between demulsification and re-emulsification upon heating to 50–60 °C then cooling overnight, respectively. This study also showed that controlled biocatalytic activation of KYpF gave more ordered structures than the use of KYF peptide per se, with less entangled slightly thicker fibres (~4.6 nm) formed.

Another triggering approach for self-assembly of the diphenylalanine-based tripeptide emulsifiers FFX (where X is a hydrophilic residue, such as S, F, D or H) that failed to form nanofibres at the oil/water interface (Scott et al. 2016), involved the conjugation of the organometallic moiety ferrocene (Fc) to the tripeptide sequence (Table 13.2) (Yang et al. 2017). The biocompatible moiety increased peptides hydrophobicity as well as steric bulk and imparted redox power to the peptide system. Taking FFH as example, the peptide failed to stabilize emulsion formation; however, the amphiphilic Fc-FFH conjugate monomers gathered at the ethyl acetate/phosphate buffer (pH 7.2) interface into thin shells (Yang et al. 2017). This orientation stabilized the fabricated nanoemulsion, which is composed of hollow nanovesicles (100–200 nm), for more than 4 months at ambient conditions

and exhibited high thermostability at 70 °C. This perfect stabilization efficiency was due to an enthalpy-controlled equilibrium among the association energy within the self-assembled peptide structure and the interfacial free energy between the peptide monomers and solvent. Other Fc-FFX sequences also successfully stabilized the nanoemulsions (Yang et al. 2017). Interestingly, tailoring the nanoemulsion droplet size, its physical appearance and its redox, as well as catalytic activity, was performed through adjusting the ratio of solvents, temperature, oxidation state of Fc group and the sequence of tripeptide. Moreover, oxidation of the ferrocene peptide-based nanoemulsion led to emergence of small micellar structures that can be employed as drug delivery vehicle. Increasing the water to organic solvent ratio led to conversion of emulsion size from microscale to nanoscale with transparent appearance. Rising the temperature of the systems to 70 °C did not cause phase separation, but only increased droplet size was observed. However, upon cooling below 25 °C, Fc-FFH emulsion showed transition into hydrogel due to reduction of monomers' aqueous solubility after cooling and increasing the association energy, which led to change of peptide conformation. Fc-FFH monomers reorganized themselves or dissociated from the interface followed by their assembly into twisted β-sheet fibres and then nanostructured hydrogels, where the FTIR of nanoemulsion showed an unstructured system (Peak at 1654 cm^{-1}), while hydrogel had a characteristic β-sheet peak at 1629 cm^{-1}. It has also been reported that His-based peptides can perform like an artificial hydrolase enzyme (Garcia et al. 2017; Wang et al. 2016; Huang et al. 2013; Guler and Stupp 2007). Based on this, Yang et al. found that Fc-FFH nanoemulsion was able to hydrolyse *p*-nitrophenyl butyrate (PNPB) into PNP, so Fc-FFH nanoemulsion also acted as an ideal artificial hydrolase enzyme with better storage stability than enzymes (Yang et al. 2017).

Other N-capped short aromatic peptides showed to stabilize foam systems, where Li et al. reported that naphthyl derivatives of the short aromatic dipeptide FF (NapFF and BrNapFF) self-assemble into thin interfacial films of β-sheet fibrous structure at the air/water interface using drop-casting technique (Table 13.2 and Fig. 13.3a–c) (Li et al. 2014). The peptide was dispersed in alkaline solvent (pH >10) where wormlike micellar structure formed followed by its dropwise addition onto a low pH solvent, leading to formation of woven strands of β-sheets configuration. The creation of interfacial self-assembled film required high peptide concentration (>0.35 wt%) besides quick protonation of peptide achieved by adjusting the subphase pH to be less than the pKa of the dipeptides, which was 3.5 and 2 for NapFF and BrNapFF, respectively. The β-sheet strands were in nanoscale width (40 nm) and when carboxylate group become protonated, bundled together to generate elastic fibres of 800 nm in thickness. They displayed an episodic wrinkle when compressed in a Langmuir trough conferring stabilization of large air bubbles for numerous days, with no coalescence or Ostwald ripening was observed. On the other hand, BrNapAV failed to build interfacial films at any concentration and different pH values although it exhibited β-sheet arrangement at high pH. This might be ascribed to the type of micelles (spherical micelles) formed at high pH differed from that formed with NapFF and BrNapFF (wormlike micelles) or the lower hydrophobicity of BrNapAV.

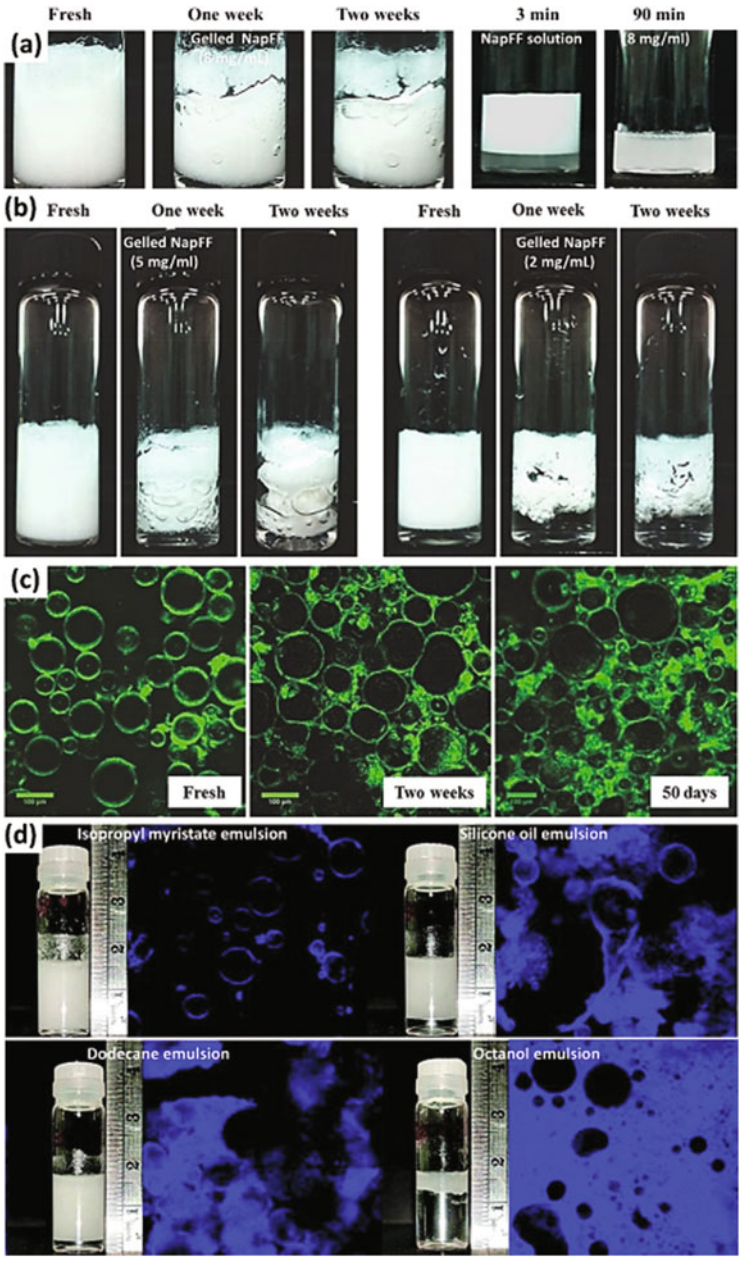

Fig. 13.3 Stabilization of foam using different NapFF concentrations, (**a**) 8 mg/mL, left, after adding $CaCl_2$, Right, without $CaCl_2$. (**b**) 5 and 2 mg/mL. (**c**) Confocal images of the air bubbles in foam showing non-spherical shapes upon bubbles distortion. Adapted from (Li et al. 2016), with copyrights permission from John Wiley and Sons. (**d**) Characteristics of four emulsions stabilized by 2 mM 2NapFF at 50 °C and the dipeptide were dyed with Nile blue in the confocal images. Adapted from (Aviño et al. 2017), with copyrights permission from Royal Society of Chemistry

The same group used the hydrophobic dipeptide NapFF (0.8 wt%) to formulate self-assembled viscoelastic hydrogel in presence of Ca^{2+} ions that can generate wet foams and stabilize them for more than 2 weeks (Table 13.2 and Fig. 13.3a) (Li et al. 2016). Due to interchain H-bonding, hydrophobicity of NapFF as well as external stimulation by cationic metals, the aromatic dipeptide self-assembled at the air/water interface into β-sheet oriented fibrous network films and stabilize the foam bubbles. The formed fibre (200 nm width) at the air/water interface (Li et al. 2016) was found to be thicker than fibres obtained from the drop casting method (40 nm width) (Li et al. 2014). In addition, the extra dipeptide moieties self-assembled in the bulk continuous phase forming a 3D structured hydrogel with high storage modulus (Li et al. 2016). Such viscoelastic hydrogel could arrest the migration of bubbles, and hence delay bubble size growth, as well as lower the liquid drainage out of the system pointing out the great stabilization of the formed foam. However, upon foam cessation, part of the aqueous phase separated from the hydrogel (Fig. 13.3a). On the other hand, the NapFF solution that was not treated with Ca^{2+} ions did not form a gel and so produced a very weak foam that ceased in less than 2 h (Fig. 13.3a) (Li et al. 2016).

Interestingly, system stabilization was shown to be concentration dependent, which might be enhanced by increasing the dipeptide concentration. For instance, 0.2 wt% NapFF formed thin fibres that collapsed in 7 days, while 0.5 wt% led to better stabilization where water leakage out of the system, reduction in foam volume and phase separation happened within 2 weeks (Fig. 13.3b, c) (Li et al. 2016). However, increasing peptide concentration to 0.8 wt% formed stable wet foam hydrogel system for more than 2 weeks (Fig. 13.3a) (Li et al. 2016). Moreover, the type of metal cation affected foam stabilization, where divalent cations can develop stiffer hydrogels than monovalent ones (Li et al. 2016; Chen et al. 2011a). In the view of this, it was found that foam induced by $CaCl_2$ addition was more stable (no coalescence) than $MgSO_4$/$MgCl_2$ followed by KCl that showed higher bubbles coarsening rate due to the absence of crosslinked fibres and presence of thin fibres 10 nm (Li et al. 2016).

Aviño et al. used extremely low concentration of 2NapFF (0.1 wt%) with two different $MgSO_4$ concentrations (18 and 142 mM) to induce self-assembled hydrogel for stabilizing foam and emulsions of different oils (Table 13.2) (Aviño et al. 2017). Micellar structure was formed after dissolving the peptide at high pH (11 ± 0.5) that converted to hydrogel after adding salt. The fibrous structure formed at the air/water interface upon adding salt to low dipeptide concentration was very loose that failed to hinder bubbles ripening leading to a weakly stabilized foam (Aviño et al. 2017). At low salt concentration, better foam quality was formed compared to higher salt concentrations, but both foams collapsed only after 2 h due to the preferential interfacial adsorption of the nanofibres leading to the weakness of the hydrogel in the bulk phase. A different behaviour was observed at the oil/water interface, where significantly more stable long-standing emulsions were produced with both $MgSO_4$ salt concentrations upon testing three different oils, isopropyl myristate, dodecane and silicone oils, while only octanol failed to be emulsified due to peptide accumulation in the oil and poor wetting of the interface

(Fig. 13.3d). The isopropyl myristate-based emulsion was the optimum formulation with no obvious creaming due to the formed interfacial film that greatly stabilized the system. However, in case of silicone and dodecane oil-based emulsions, stabilization was only attributed to hydrogel formation in the continuous phase, as well as wetting properties of peptide at the interface. To that end, it could be concluded that gelation of naphthyl derivatives of short aromatic peptides is possible by dissolving the peptide in an alkaline medium then adding salts or lowering the pH.

13.2.2 α-Helix Peptide Emulsifiers

Bioinspired short amphiphilic peptide sequences that have tendency to acquire α-helical structures at organic/aqueous interfaces have been widely studied for their surface activity and emulsification capacity. For instance, the surface activity, conformational rigidity and helical propensity of the fungal structural hydrophobin proteins inspired the development of a library of short biotriggered helical emulsifiers, by Gazit and co-workers (Mondal et al. 2017). The helical heptad amphipathic peptides showed to stabilize silicon oil-based O/W emulsions. The design was based on the incorporation of the helical-forming non-proteinogenic amino acid, α-aminoisobutyric acid (Aib), at positions (i, i + 3), which enabled the formation of supramolecular helical structure both in aqueous phase and at oil/water interface (Fig. 13.4a). The parent peptide of this library was designed by modifying the previously reported helix-forming peptide, SHR-FF peptide (Ser-Aib-Phe-Ser-Aib-Phe-Aib) (Mondal et al. 2015), into SHR-FLLF (*Phe*-Aib-*Leu*-*Ala*-Aib-*Leu*-*Phe*) (Table 13.2). The terminal Phe groups of one strand allowed the π–π stacking with another adjacent one, while Leu inclusion offered zipper conformation via hydrophobic bonding in addition to increasing hydrophobicity by adding alanine instead of serine (Fig. 13.4a) (Mondal et al. 2017). Such structural modulation favoured the self-assembly into highly ordered supramolecular aggregates of helices, forming cylindrical micelles-like nanofibres (Fig. 13.4a) (Mondal et al. 2017). It was postulated the presence of 2 asymmetric structural units: (A) right-handed α-helix and

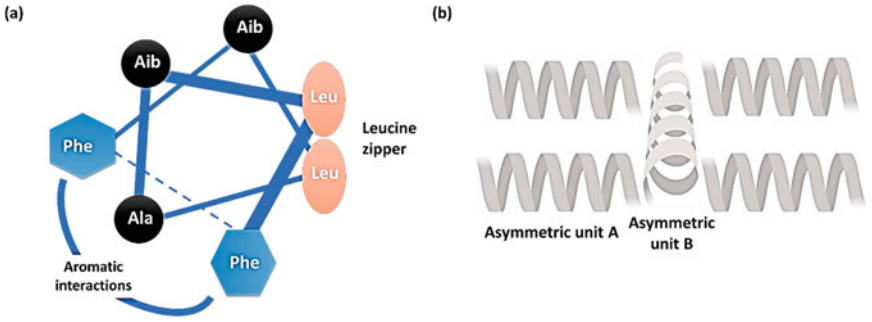

Fig. 13.4 (**a**) Helical wheel representation and (**b**) perpendicular packing pattern of SHR-FLLF

(B) 3_{10}-helix, due to intrahelical H-bonding, with perpendicular orientation of unit A to B triggering hydrophobic and π stacking interactions forming knob-into-hole arrays (Fig. 13.4b) (Mondal et al. 2017). This arrangement created a helical hydrophobic column with dual hydrophilic terminals similar to bolaamphiphiles. SHR-FLLF showed to act as a biosurfactant at concentrations of 5, 10 and 15 mg/mL (critical assembly concentration, CAC = 2.8 mg/mL), emulsifying silicone oil in water (pH <2) forming O/W emulsions. The lowest peptide concentration (5 mg/mL) demonstrated stability for >1 week which was comparable to the commercial anionic surfactant sodium dodecyl sulphate (SDS), whereas higher concentrations (10 and 15 mg/mL) showed at least 2-month stability and some formulations did not show any signs of phase separation for up to 8 months. SHR-FLLF-based emulsions displayed highly charged droplets with similar emulsion properties to SDS due to the helical arrangement at the interface, in addition to interfacial self-assembly ensuring its strong surface activity. Additionally, emulsions formed at 10 and 15 mg/mL peptide concentrations demonstrated viscoelastic characteristics preventing phase separation, due to high viscosity of the formulations. The Tween 20-emulsified system showed larger droplet size than the SHR-FLLF peptide-based emulsions, leading to creaming and phase separation in 48 h. The replacement of alanine with a charged amino acid either glutamic acid or lysine (SHR-FLELF and SHR-FLKLF) was examined, which aimed to break the bolaamphiphilic behaviour while retaining helical propensity. Both charged analogues acquired the α- and 3_{10} helical structures in water, where SHR-FLELF self-organized forming a micellar arrangement, while SHR-FLKLF stayed in unaggregated form. Consequently, SHR-FLKLF (5 and 7.5 mg/mL) stabilized the emulsion for less than a week, while the SHR-FLELF-based emulsion showed longer stability (>2 months at concentrations of 7.5 and 10 mg/mL) with viscoelastic shear-thinning behaviour.

A bioinspired switchable amphiphilic helical peptide emulsifier, Lac21, was also designed by the Middelberg's group, which mimic the bacterial Lac repressor DNA-binding protein (Dexter et al. 2006). The Lac21 amphiphilic peptide (Ac-MKQLADSLMQLARQVSRLESA-$CONH_2$) is a hydrophilic heptad repeating motif *abcdefg* containing hydrophobic amino acids at the *a* and *d* positions spaced by alternating 3 and 4 amino acid residues of the bacterial Lac repressor protein sequence, with acetylated and amidated C- and N-terminals, respectively, to prevent interpeptide charge–charge interactions (Fig. 13.5) (Dexter et al. 2006). Lac21 did not form organized structure in water; however, it could adsorb and adopt a supercoiled α-helix structure at organic/aqueous and air/aqueous interfaces in a monomeric free "detergent" state reducing interfacial tension, in a similar behaviour to low molecular weight surfactants (Fig. 13.5) (Dexter et al. 2006). Despite the interfacial adsorption and helical structure formation, Lac21 failed to stabilize foams and emulsions as it lacks the ability to form interfacial cohesive film, although it is derived from protein that could form interfacial films. Interestingly though, Lac21 peptide was used as a parent sequence for the design of a library of peptides exhibiting robust intermolecular crosslinking at the interface generating stable cohesive interfacial films.

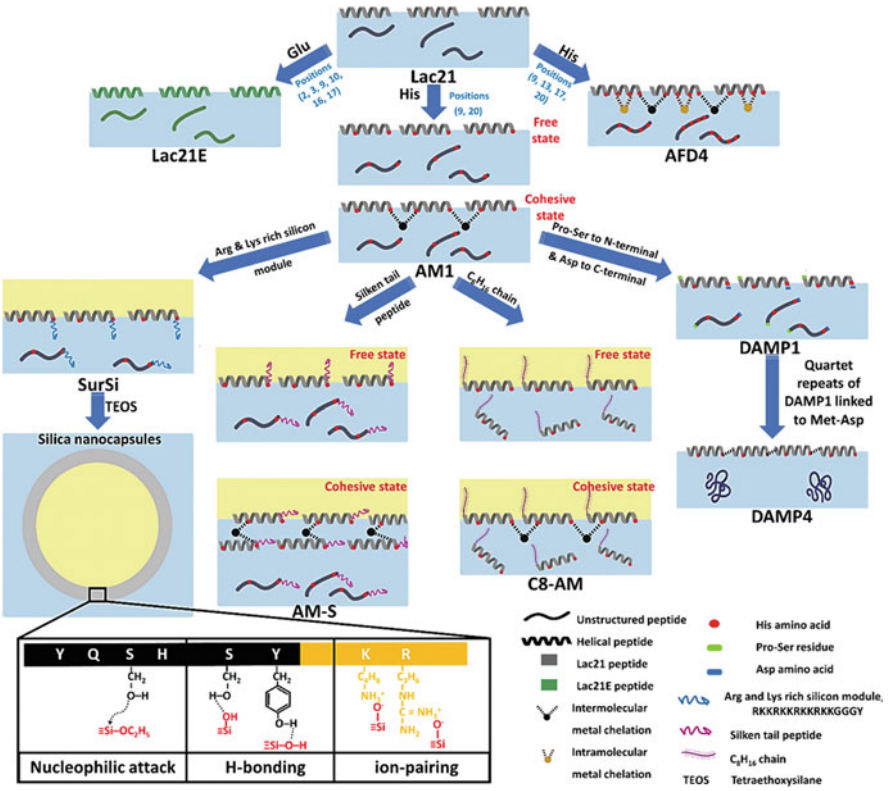

Fig. 13.5 Self-assembly of α-helix-forming peptides (Lac21 and its derivatives) in bulk phase and at interface

One example of these peptides is the 21-residue peptide AM1, which is a Lac21 sequence mutated with histidine (H) residues at positions 9 and 20 (Ac-MKQLADSL*H*QLARQVSRLE*H*A-$CONH_2$). AM1 showed to form and stabilize foams as well as 20%v/v toluene/water emulsions upon changing the composition of the continuous aqueous media using metal cations and by tuning pH to 7.4 (Table 13.2) (Dexter et al. 2006). This peptide adsorbed at fluid–fluid interface acquiring α-helical structure in a detergent mobile state where the hydrophobic moieties were directed towards the interface exhibiting interfacial tension lowering property like Lac21 (Fig. 13.5) (Dexter et al. 2006). However, the interfacial tension reduction due to AM1 occurred more rapidly than Lac21, which is attributed to the less organized structure of AM1 (random coil monomers) in bulk phase due to replacing the high helix-forming methionine (M) at position 9 in Lac21 with low helix-forming H residue. Such modification decreased the energy barrier against the adsorption of AM1 and led to its arrangement in α-helical structure at the interface. Interestingly, the H residues at positions 9 and 20 were oriented towards the bulk hydrophilic phase (Fig. 13.5) (Dexter et al. 2006). These residues bind to

metal ions (100 μM Zn^{2+}) at neutral pH allowing intermolecular crosslinking of the peptides located at the interface without metal binding in the bulk (Fig. 13.5) (Dexter et al. 2006). The interfacial assembly of AM1 developed a monolayer of a cohesive mechanically rigid film with elasticity modulus 121 mN/m comparable to the protein's interfacial film, and no major effect on the lowered interfacial tension was recorded after metals. Additionally, the great spacing between the H residues in same sequence prohibited the intramolecular crosslinking using metal ions.

Treating of the AM1-based system with chelating agent (EDTA) or protonation of H residues by acidification to pH 3.6 did not change the interfacial tension but reversed the film state into the starting loose form (elasticity modulus <30 mN/m) in seconds due to abortion of crosslinking leading to emulsion break down and foam collapse. Adding excess metal ions or neutralizing the medium pH could return the interfacial peptides into their coherent film again and stabilize the system. AM1 stabilized the foam for about 10 min which collapsed within 1 min after acidification or metal sequestration by EDTA (Dexter et al. 2006). Such switchable behaviour of AM1 allowed a novel and easy demulsification technique for clean oil and water recovery without residues in any phases, which is better than other energy consuming and ineffective approaches. In another study, Dexter and Middelberg compared the effect of various metals on the strength of the formed interfacial film, where Zn^{2+} was the best crosslinker followed by Ni^{2+} and then CO^{2+}, while Ca^{2+} and La^{3+} failed to create interfacial bridges, implying the different binding behaviour of metals that can influence film formation and the characteristics of formed films (Table 13.2) (Dexter and Middelberg 2007).

Middelberg et al. also compared between Lac21E (Ac-M*EE*LADSL*EE*LARQV*EE*LESA-NH_2) and AM1 for foam stabilization (Table 13.2) (Middelberg et al. 2008). Lac21E formed a strong elastic interfacial layer of organized connected α-helices at pH 3 (close to isoelectric point 3.95) with lowered interfacial tension (ON state), followed by interfacial disassembly and dissociation from the interface into the bulk medium upon neutralizing the pH to 7.4 due to acquiring a high negative charge and loss of interfacial activity and elasticity (OFF state) that was reversed again by reacidification. So, Lac21E stabilized foams for 5 min at pH 3 but collapsed within 1 min at pH 7. The film formed by Lac21E was stronger than AM1 due to greater accumulation of Lac21E at the interface.

Another Lac21 peptide analogue reported by Dexter and Middelberg is AFD4 (Ac-MKQLADS L*H*QLA*H*KVS*HLEH*A-$CONH_2$), in which 4 H residues are present at positions (i, i + 3) and (i, i + 4) to endorse intramolecular crosslinking with 'metal clip'via sequential α-helical peptide turns to further stabilize the helix, in addition to the interfacial intermolecular bridging (Fig. 13.5 and Table 13.2) (Dexter and Middelberg 2007). Unlike Lac21 and AM1, AFD4 caused a more rapid decline in interfacial tension in the absence of metal ions, since substitution of R with H residue at position 13 widely destabilized the helical form in the bulk phase besides the electrostatic repulsion between cationic amino acids. Addition of metal ions to AFD4-based systems was found to reduce surface tension at a slower rate due to the slower adsorption kinetics after crosslinking in the bulk phase into higher helical

structure (Fig. 13.5) (Dexter and Middelberg 2007). AFD4 yielded tougher cohesive films at the interface after metal incorporation than AM1 at same environmental conditions, which demonstrated to be as strong as the lysozyme and β-lactoglobulin films. The effect of metal ion type on AFD4 film strength was similar to AM1, where Zn^{2+} constructed the strongest intermolecular bridge, whereas Ni^{2+} allowed the most stable helix. Like AM1, AFD4 film could be simply switched to detergent state using EDTA or acidification. Foam stabilization property was studied for the three peptides (Dexter and Middelberg 2007), where Lac21 showed to reduce interfacial tension without bubble stabilization both in the presence and absence of metal ions. While AM1 failed in the absence of metal ions to stabilize foam with low foam height after 25 min (3 mm), which slightly increased after metal addition. Same behaviour was observed for AFD4, but the metal addition significantly increased the foam height to 50–53 mm after 25 min and the AFD4-Zn^{2+} systems stabilized the foam for more than 1 h without collapse.

Wibowo et al. introduced the helix-forming peptide AM-S, which is a modified analogue of the peptide bioemulsifier AM1, by conjugating a silken tail peptide inspired from *Bombyx mori* silkworm fibroin, which is composed of eight hydrophobic amino acid sequence of alternating G and A using *PS* residues as linkers (Ac-MKQLADS LHQLARQ VSRLEHA-*PS-GAGAGAGY-CONH*$_2$) (Fig. 13.5 and Table 13.2) (Wibowo et al. 2017). AM-S combined the AM1 features of facial amphiphilicity, interfacial activity as well as crosslinking ability in the presence of metal ions, in addition to improved air/water interfacial adsorption capability of silken tail, thus maintaining optimum rate of interfacial adsorption and enhancing interfacial stability. The P and S residues of the linker sequence provided free rotation of strands. As discussed earlier for AM1, AM-S peptide also exhibited a random coil structure in aqueous phase with quick diffusion to the interface lowering the interfacial tension to 52 mN/m using 10 μM peptide, which was not changed by introducing $ZnCl_2$. AM-S created interfacial multilayers of self-associated α-helical conformation rather than the monolayers produced by AM1 due to the hydrophobic bonding between molecules after the silk tail addition (Fig. 13.5). Interestingly, the thickness of AM-S/Zn^{2+} films was higher than AM1 one because of the peptide multiple layering, so greatly resisted desorption from the interface upon compression and stabilized the dense foams containing miniaturized bubbles (Wibowo et al. 2017). However, AM-S interfacial adsorption kinetics was slower than AM1 owing to its increased molecular weight by silk tail. Both AM1 and AM-S could not stabilize the foam, which collapsed within 2 min while they expressed film stability in the presence of $ZnCl_2$ due to film elasticity without increase in bubble size.

Wang and co-workers constructed another derivative of AM1, C8-AM, which is AM1 peptide sequence capped from N-terminus by a C8 hydrocarbon chain, which is a hydrophobic functionality for enhancing its interfacial anchoring propensity (Table 13.2) (Wang et al. 2017). In comparison to AM-S, C8-AM acquired an α-helical conformation in bulk phase rather than the random coiling of AM-S, where the latter only assembled at the interface and did not form micelles in bulk, but only soluble dimers to tetramers. C8-AM (20 μM) adsorbed at oil/water interface

at a slower rate than AM-S, due to its ordered helical structure in bulk in addition to the hydrophobic interaction between C8 chains. In the absence of Zn^{2+}, C8-AM reduced interfacial tension to 8.4 mN/m within 400 s compared to 17 mN/m in case of AM-S. In the presence of Zn^{2+}, C8-AM crosslinking happened via H residues forming a cohesive interfacial film (Fig. 13.5). After treatment with EDTA, C8-AM-based emulsion was disrupted after 6 hours while AM-S emulsion broke down within 20 min due to the robust binding of C8 groups to the interface even after interrupting the metal ions-mediated crosslinking. Interestingly, C8-AM created 2% Miglyol 812-based O/W nanoemulsion of smaller globular size (147 nm) than AM-S (180 nm) after sonication, where a concentration of 100 μM of C8-AM was enough to stabilize the system for 3 weeks, whereas higher concentration of AM-S (400 μM) was required to achieve equivalent stabilization. Unlike AM-S, C8-AM did not show flexible reversibility at the interface due to rigid binding of C8 hydrophobic group to the interface.

Middelberg and co-workers deigned a novel bifunctional peptide SurSi (Ac-MKQLAHSVSRLEHA-*RKKRKKRKKRKKGGGY-CONH$_2$*), by conjugating the R- and K-rich peptide segment, Si module (RKKRKKRKKRKKGGGY), to AM1 (Wibowo et al. 2014). Hui et al. made further study on SurSi, which revealed the ability of this peptide to stabilize nanoemulsion at 400 μM concentration for at least 2 weeks (Table 13.2) (Hui et al. 2016). Furthermore, the ability of coating oil droplets by silica shell was investigated, in order to formulate stable oil-filled nanocapsules near neutral pH at ambient conditions with no harmful ingredients showing sustained release property for the entrapped drugs (Wibowo et al. 2014). AM1 peptide could not perform this function where precipitation of silica occurred in continuous phase not at the interface, forming irregular aggregates. On the other hand, SurSi successfully created the nanocapsule, as the dual functionalized peptide combined the surface active AM1-derived moiety responsible for nanoemulsion formation with the R- and K-rich Si module, which developed biosilicification at oil/water interface (Fig. 13.5). The modulated AM1 moiety contained solely the first and last heptads of the parent AM1, while D at position 7 in the first heptad was replaced with H to retain the metal binding capacity for crosslinking at the interface to enable the formation of cohesive films. The use of 2 heptads only instead of 3 was to enhance interfacial adsorption, as there is an inverse relation between the peptide molecular weight and the square of interfacial adsorption rate (Middelberg et al. 2000).

SurSi interfacial activity and surface coverage were very low at neutral pH as compared to AM1, due to the delayed diffusion to the interface resulting from the strong repulsive forces between peptide chains (theoretical charge = 13.44), leading to large spacing between the strands and hence lack of interfacial film formation even upon adding Zn^{2+}. However, neutralizing the charge through increasing the pH could enhance the adsorption kinetics and interfacial activity of SurSi. Indeed, SurSi peptide successfully emulsified Miglyol 812 oil containing oil-soluble moiety (fipronil) in water at neutral pH 7.5, forming nanoemulsion of droplet size 66.5 nm, which was larger in size, lower in zeta potential and less stable than AM1-based emulsion. Increasing the peptide concentration had a positive effect

on reducing the droplet size of emulsion (Hui et al. 2016). The addition of tetraethoxysilane (TEOS) to the system produced silica nanocapsules after 20 h via different mechanisms (Fig. 13.5). It was suggested that E, Y, S and H residues hydrolysed TEOS via nucleophilic attack on silicon atom resulting in silanolate anion and silanol (Wibowo et al. 2014). Furthermore, silanolate anions developed electrostatic attraction with the cationic residues K and R, in addition to the H-bonding between silanol, as well as with hydroxyl groups of Y and S. Silanolate anion and silanol acted as nuclei inducing further silica precipitation. The thickness of nanocapsules shell could be amplified by elevating pH to increase the levels of silanolate, reaction time and levels of TEOS (silica species precursor) to slow the release rate of entrapped compounds.

Middelberg and Dwyer crosslinked four AM1 peptides via DPS short peptide linker to enhance folding propensity, developing a soluble and stable protein emulsifier DAMP4 [M*D*(*PS*M*K*QLADSLHQLARQ-VSRLEHAD)$_4$] (Table 13.2) (Middelberg and Dimitrijev-Dwyer 2011). The D anionic residue induced repulsive forces between strands and P would terminate helix formation, whereas S residue supported the free rotation. The cationic K residue was deprotonated at pH 8.5, so DAMP4 acquired a single negative charge and stabilized the foams created, while decreasing pH by 1 unit (pH 7.4) expedited the foam collapse due to neutralization of the charge, though there was no change of its effect on interfacial tension at both pH values. Destabilization effect of divalent cation Ca^{2+} on the foam formed at pH 8.5 was higher than that of the monovalent Na^+, due to greater charge screening effect of Ca^{2+}. Interestingly, the use of kosmotropic electrolyte such as Na_2SO_4 salt was able to share the intrinsic surface hydration layer of DAMP4 and support the foam stability at pH 7.4 where DAMP4 net charge was zero. Na_2SO_4 salt allowed the electrostatic interaction of SO_4^{2-} ion to the basic residues of DAMP4 (R and K), resulting in amplified repulsive force 'hard-sphere repulsion', as well as highly oriented robust hydration film and better foam stability (Middelberg and Dimitrijev-Dwyer 2011; Parsons and Ninham 2010; Tavares et al. 2004; Besseling 1997). On the other hand, the chaotropic salt (NaSCN) does not have a tightly held hydration layer and debilitate the hydration layer of DAMP4 (Middelberg and Dimitrijev-Dwyer 2011; Gao et al. 2009).

In a further study, Dwyer and co-workers investigated the influence of molecular size of peptides and proteins and their bulk structure on their respective interfacial activities, by comparing the long well-organized protein DAMP4 to its simple unorganized peptidic precursor DAMP1 as well as studying their mixture (Table 13.2) (Dwyer et al. 2013). DAMP1 was a slightly modified form of AM1 via adding P and S residues to the N-terminus and a D residue to the C-terminal (*PS*MKQLADS-LHQLARQVSRLEHA*D*), while DAMP4 was the quadriad form of DAMP1 with the inclusion of a M and D to N-terminus [MD(PSMKQLADS-LHQLARQ-VSRLEHAD)$_4$]. The unstructured DAMP1 adsorbed quickly to the air/water interface as monomers of α-helices whereas DAMP4, as mentioned before, formed a robust package of 4 helices, so it was slowly attracted to the interface after unfolding into a chain of engaged DAMP1 forming interfacial monolayers and recording greater interfacial elasticity (Fig. 13.5). Both the peptide and protein

quantities were identical at bulk and interface indicating that adsorption energy was affected by the chemical structure only rather than the size which only influenced the adsorption rate. Strikingly, a faster interfacial tension drops upon mixing DAMP1 and DAMP4 compared to individual components, implying augmentation effect of the mixture surface activity.

Inspired by DAMP4 molecular design, Zhao et al. developed the anionic protein emulsifier SP16 [MD(*P*-*S*-ANSVAESLANLAESVSELVSNA-*D*)$_4$] to create and tailor foams, which can be controlled by pH and ionic strength (Table 13.2) (Zhao et al. 2017). SP16 is composed of four repeats of one peptide sequence linked by an acid cleavable sequence DP followed by S residue as a spacer. The hydrophobic part of the structure maintained the 4-helix bundle conformation, implying heat resistance property besides the hydrophilic and hydrophobic faces created by the orientation of amino acids which guaranteed the surface activity of SP16. Being anionic in nature, SP16 had a very low isoelectric point (pI) of 2.98, leading to the high pH responsiveness of the folded structure and hence the foaming properties. Minor foam formation was achieved at the pI, but altering the pH above or below pI by 1 pH point led to folding of SP16 into helix bundle followed by quick interfacial adsorption, as well as reduction of interfacial tension with enough charge to stabilize foam formation. Increasing the pH to 6 and above, negatively charged the protein hindering its folding, consequently decreased interfacial adsorption propensity and disrupted the orientation of hydrophilic and hydrophobic residues at the interface as well as surface activity, though charge screening by NaCl recovered the foaming activity. Interestingly, at pH 5, SP16 was able to fold into helix bundle in the bulk; however, due to its high negative charge there was a delay in interfacial adsorption behaviour leading to weak foam formation, unless NaCl was added.

Besides the hydrophobin and Lac analogous peptides, other designs of α-helical peptide emulsifiers were reported. For instance, anionic poly(γ-benzyl L-glutamate)$_n$ polypeptides (PBLG) were developed by Morikawa and co-workers, with different polymerization numbers (1a, $n = 12$ and 1b, $n = 32$) (Table 13.2) (Morikawa et al. 2005). PBLGs could self-associate into α-helical robust rods and form O/W microemulsion (CH_2Cl_2/water = 1:2 or CH_2Cl_2/methanol/water = 1:1:1, v/v), which were used as templates for formulation of stable hollow microcapsules upon evaporation of the volatile organic phase, a system that could be used to deliver both hydrophilic and lipophilic drugs. Only 68% of the shorter oligopeptide 1a formed α-helices in the emulsion (with the appearance of some β-sheet structure after air drying), while the longer one 1b had 97% of α-helix conformation confirming that longer sequences provided more helical propensity. The amphiphilic polypeptide was adsorbed to the organic/aqueous interface and upon evaporation more monomers were attracted to the interface forming small multilayered microcapsules of assembled peptides (1–5 μm) containing aqueous phase in the core. These microcapsules were able to entrap a hydrophobic molecule (pyrene) via binding to the shell. The dichloromethane emulsion showed aqueous layers separation after 5 min and the emulsion layer contained droplets of 5–60 μm in size. Adding methanol to the system decreased the droplet size within 3 min to <10 μm and enabled longer stabilization for 24 h before separation of aqueous layers.

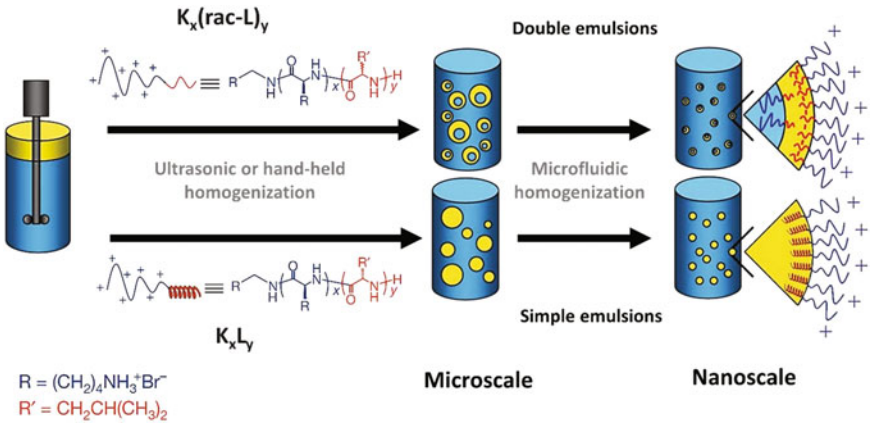

Fig. 13.6 Emulsification technique to generate both simple and double emulsions by block copolypeptide surfactants. Adapted from (Hanson et al. 2008), with copyrights permission from Springer Nature

Amphiphilic diblock copolypeptide emulsifiers were also developed by Hanson et al., with N-terminus hydrophilic block formed of cationic poly-L-lysine sequence (20–100 residues) conjugated to a hydrophobic racemic leucine (rac-L) sequence (5–30 residues) from the C-terminus (Fig. 13.6) (Hanson et al. 2008). The surfactant-like design imbued the polypeptide with surface activity and interfacial stabilization ability owing to the amphiphilicity and intermolecular H-bonding. These emulsifiers $K_{20}(rac\text{-}L)_{10}$, $K_{40}(rac\text{-}L)_{10}$, $K_{40}(rac\text{-}L)_{20}$, $K_{40}(rac\text{-}L)_{30}$, $K_{60}(rac\text{-}L)_{20}$ and $K_{100}(rac\text{-}L)_{10}$ could develop W/O/W double emulsions (Table 13.2 and Fig. 13.6) via easy homogenization and microfluidic techniques without the aid of other emulsifiers, as well as providing long-term stabilization for the formed emulsions (>9 months), while the less hydrophobic emulsifiers (5 residues of rac-L) stabilized the system for 12 months with bigger droplet size. The use of hand operated homogenization or ultrasonic mixing yielded microemulsion which was converted to nanoemulsion after microfluidic homogenization (Fig. 13.6). The flexibility of orientation of rac-L chain in diblock copolypeptide enhanced its solubility in oil with minimal interchain H-bonding and packing and hence weakly stabilized the inner water globules in the external oil phase. However, on the outer oil/water interface, intense packing of the rac-L in oily phase resulted in strong crosslinking by H-bonding that inhibited the conversion into a simple emulsion and stabilization of the double emulsion without inclusion of other additives. Interestingly, the $R_{40}(rac\text{-}L)_{10}$, $E_{40}(rac\text{-}L)_{10}$, $K_{60}(rac\text{-}V)_{20}$ and $K_{60}(rac\text{-}A)_{20}$ also stabilized double emulsions due to structure similarity to $K_x(rac\text{-}L)_y$, with the flexibility of design versatility (Table 13.2 and Fig. 13.6). On the other hand, the $K_{60}L_{20}$ emulsifier only produced simple O/W emulsions owing to the low solvation of the homochiral L-leucine part in oil phase upon acquisition of α-helical structure, while the hydrophilicity of the homopolypeptide block K_{60} favoured rapid phase separation

(Table 13.2 and Fig. 13.6). Thus, for this type of emulsifiers, the interfacial helical propensity impaired surface activity rather than enhancing it.

13.2.3 β-Sheets Peptide Emulsifiers

β-sheet forming peptides have been widely studied for the development of amyloid-like nanofibrous structures for the formation of hydrogels in aqueous media (Wychowaniec et al. 2020; Gazit 2007; Aggeli et al. 2001; Zhang et al. 1994). In addition to hydrogelation properties, amphiphilic β-sheet forming peptides have been shown to possess interfacial activity (Fig. 13.7a). Dexter was the first to introduce amphiphilic β-strand peptides as emulsifying agent that adsorbed from bulk to the interface (Dexter 2010). Inspired by the β-sheet forming amphiphilic sequence design of the Tirrell group that form monolayer at the air/water interface (Rapaport et al. 2000), Dexter developed the following four short nonapeptides B-14 (Ac-PDFDFDFDP-$CONH_2$), B-15 (Ac-PHFHFHFHP-$CONH_2$), B-16 (Ac-PEFEFEFEP-$CONH_2$), and B-17 (Ac-PKFKFKFKP-$CONH_2$) of alternating hydrophobic residues (P or F) with same charged residues, which are either anionic (E, D) or cationic (K or H), to hinder any possible electrostatic crosslinking of the β-sheets in bulk phase and aid in the interfacial adsorption (Table 13.2 and Fig. 13.7b) (Dexter 2010). These peptides showed surface activity at different pH values in a similar manner to traditional ionic emulsifiers, but with good biocompatibility and biodegradability. When the peptide was uncharged by adjusting the pH of B-14 and B-16 to acidic or B-15 and B-17 to basic, it acquired β-hairpin conformation rather than β-sheet in bulk phase, owing to the aromatic interaction of F residues at positions 3 and 7. Formation of strong rigid film of peptide aggregates at the interface is mediated by H-bonding and hydrophobic interactions, forming emulsion with large droplet size ~1500 ± 100 nm except for B-17 (~400 nm) due to the reduced zeta potential which allowed coalescence to happen (Fig. 13.7b). Increasing zeta potential through pH change led to formation of polyproline II-form helices in bulk and decreased the interfacial spreading with better emulsification due to electrostatic repulsion, so intermediate charging of peptide was the optimum. Based on this, B-14 to B-17 could stabilize emulsions at different pH ranges; however, they were more successful as ionic emulsifiers than film forming emulsifiers. The kinetics of B-14 and B-16 peptides adsorption were similar at all pH ranges, while decreasing charges of B-15 and B-17 slowed their adsorption rate due to aggregation in aqueous solution.

Another β-sheet forming peptide is the fibrillized short peptide Q11 (Ac-QQKFQFQFEQQ-Am), which was reported by Tian et al. to self-assemble at oil/water interface (Table 13.2) (Tian et al. 2011). Interfacial self-assembly of Q11 is triggered by the addition of Dulbecco's phosphate buffer saline to stabilize W/O emulsion via formation of microgel spheres surrounding the internal aqueous phase

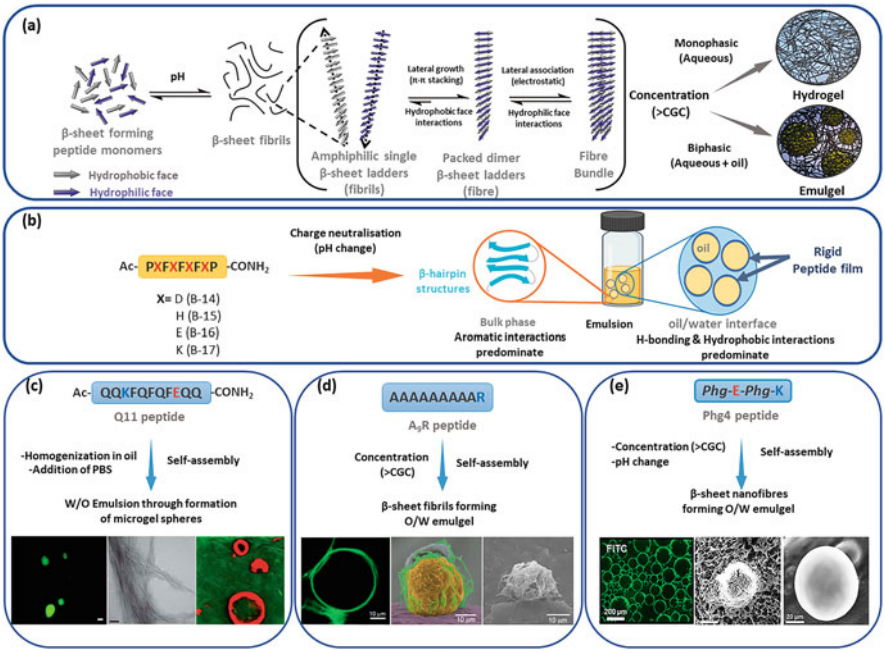

Fig. 13.7 (**a**) Schematic presentation of the general self-assembly mechanism of β-sheet forming peptides into amphiphilic β-sheet nanofibres, forming hydrogels in aqueous media and emulsions/emulgels in biphasic media. Adapted from (Wychowaniec et al. 2020), with copyrights permission from the American Chemical Society published under Creative Commons Attribution 4.0 International license. (**b**–**e**) Examples of β-sheet forming peptide emulsifiers, (**b**) Amphiphilic β-strand forming peptides; B-14, B-15, B-16 and B-17, which self-assemble at oil/water interface into rigid peptide films, stabilizing emulsion formation. Adapted from (Dexter 2010), with copyrights permission from the American Chemical Society. (**c**) Self-assembly of Q11 peptide at oil/water interface, forming W/O emulsion through formation of microgel spheres surrounding the aqueous media, Left: Fluorescent nitrobenzoxadiazole (NBD)-containing microgels produced with a paddle-type stirrer, Middle: TEM of the microgel fibrous structure (scale bar 100 nm), Right: Laser scanning confocal microscopy of Congo red-stained microgels. Adapted from (Tian et al. 2011), with copyrights permission from Royal Society of Chemistry. (**d**) Self-assembly of A_9R peptide into hydrogel in water and O/W emulsion. Left: Laser scanning confocal microscopy, Middle and Right: cryo-SEM of 0.05 wt% A_9R emulsion. Adapted from (Castelletto et al. 2019), with copyrights permission from the American Chemical Society. (**e**) Self-assembly of Phg4 peptide into β-sheet nanofibres, forming hydrogel and O/W emulgel, Left: Fluorescence microscopy of Phg4 O/W emulsion (stained with FITC), Middle: SEM of Phg4 vacuum-dried O/W emulgel, Right: SEM of Phg4 air-dried O/W emulgel. Adapted from (Wychowaniec et al. 2020), with copyrights permission from the American Chemical Society published under Creative Commons Attribution 4.0 International license

(Fig. 13.7c). It was possible to control the microgel size and size distribution using characteristics of speed and type of blade mixer, as well as further shear steps beyond the gelation. Interestingly, NIH 3T3 fibroblasts and C3H10T½ mouse pluripotent stem cells were encapsulated within the microgel spheres with acceptable

biocompatibility during the emulsion preparation process, by dispersing the cells within the peptide aqueous solution before addition of buffer for emulsification.

Surfactant-like β-sheet forming peptides were also designed to act as emulsifiers, where Castelletto and co-workers introduced the surfactant-like A_9R peptide which formed hydrogel in water and stabilized O/W Pickering emulsions, in a similar way to proteins (Table 13.2) (Castelletto et al. 2019). Unlike traditional surfactants, A_9R did not from interfacial monolayers, but rather the emulsion droplets were wrapped by a network of self-assembled β-sheet fibrils (25 nm diameter) of A_9R when exceeding the critical aggregation concentration (0.05–0.07%) without the need for pH tuning due to the strong packing of A residues in the core and surface exposure of the R residue to aqueous phase (Fig. 13.7d). The emulsion was stable by A_9R emulsifier for 3 days instead of 1 day only in absence of the peptide. On-demand demulsification was achieved by the addition of the proteolytic enzyme elastase, which could be exploited for site-specific release of entrapped drugs. In addition, A_9R showed a remarkable antimicrobial action towards G-ve bacteria including *P. aeruginosa* and *E. coli*.

Ionic self-complementary peptides are characterized by alternation of a hydrophobic residue with counter charge residues and are the most used sequences for the formation of β-sheet assembled structures. Elsawy and co-workers were the first to develop the shortest ionic self-complementary tetrapeptide Phg4 (PhgEPhgK, where Phg is phenylglycine), which can self-assemble into thermodynamically stable β-sheet nanofibres (diameter ~ 7–11 nm) that are not only capable of hydrogel formation in monophasic aqueous medium but can also stabilize O/W emulsions in biphasic media (Table 13.2) (Wychowaniec et al. 2020). Emulsification was pH and concentration dependent, where surface activity was only achieved at the assembly pH range (4.5–8) and concentration (>2%W/V). Electron microscopy (both SEM and TEM) showed the adsorption of peptide nanofibres at the oil/water interface forming nanofibrillar microspheres (∼50–200 μm) encapsulating oil droplets within the nanofibrous network of the continuous phase (Fig. 13.7e). These structural features stabilized the formation of viscoelastic emulgels, which showed to be shear thinning and thixotropic. Emulsification was pH switchable, as emulgel formation only happened at self-assembly pH range (4.5–8), where the overall charge of the peptide chain is neutral favouring both assembly and interfacial adsorption. While outside this pH range, phase separation occurred owing to the repulsion of charged peptide chains and failure to self-assemble into the emulsifier β-sheet nanofibre form. Phg4 successfully formed O/W emulgels with chloroform and melissa oil as the organic phase at a range of oil:water ratios and peptide concentrations. The peptide emulsifier stabilized melissa emulgels for longer than 5 weeks and showed to withstand harsh environmental conditions (heating at 60 °C for 3 hours and salting out for 1 week) with no signs of phase separation, which was superior to commercial emulsifiers, such as cetrimide, SDS and tween 80.

13.2.4 Miscellaneous Surfactant-Like Peptides

In addition to peptide emulsifiers that assemble into well-defined secondary structures, there has been endeavours for molecular engineering of peptides that mimic surfactant structures. One example of these emulsifiers is the synthetic pseudopeptide gemini amphiphile (GAP), which was reported by Lotfallah et al. (Lotfallah et al. 2015). GAP was designed to have a hydrophilic head of valine-derived pseudopeptide exposed to aqueous phase with 2 hydrophobic tails that solubilize in oil phase by van der Waals force with variable critical aggregation concentration (4–25 mM) depending on the ionic strength and pH of the system (Fig. 13.8). Amphiphilic GAP thus self-associates at oil/water interface forming hollow microspheres (1–5 mm in diameter), therefore stabilizing O/W emulsion containing <1% of isopropyl myristate oil, after strong mixing by magnetic stirrer for 30–90 min (Table 13.2 and Fig. 13.8). The formed emulsion displayed a superior stability against exposure to strong acids, heating at 45 °C for 4 months, mechanical stress (centrifugation for 30 min at 3000 rpm with good system recovery if centrifuged for longer time) and long-term storage. However, proteolysis with thermolysin enzyme or alkalinisation to pH 12 led to disassembly and phase separation. It was suggested that surface activity of GAP required total or partial protonation of its amino groups to stabilize the emulsion droplets, so it could be exploited as a carrier for delivery of anionic nucleic acids. The system can also be used for the encapsulation of a variety of hydrophobic compounds, which was demonstrated by the successful encapsulation of the fluorescent hydrophobic model compounds N,N-diethyldansylamide and 9,10-dimethylanthracene.

Lipopeptides also showed to exhibit good surface activity thanks to the amphiphilicity of the molecular design. The lipodipeptide emulsifier, C_{13}-KR, was purposely designed by Lv et al. to stabilize emulsions in acidic environment, where its surface activity was compared to whey protein isolate and Tween 80 (Table 13.2) (Lv et al. 2019). The peptide-based emulsion showed the smallest droplet size (<1 μm) and the largest surface charge (100 mV), electrostatic repulsion and creaming stability, compared to the emulsions formed by the other two emulsifiers.

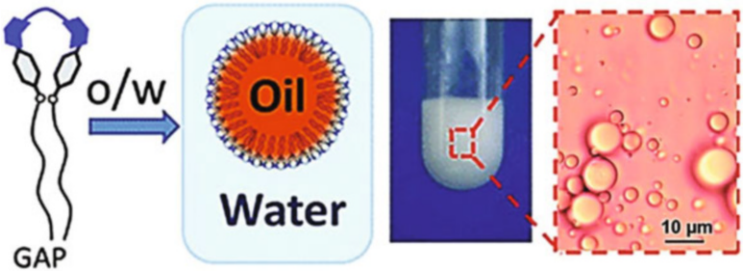

Fig. 13.8 Diagram of GAP self-assembling to form an O/W emulsion with macroscopic and microscopic images of the formed emulsion. Adapted from (Lotfallah et al. 2015), with copyrights permission from Royal Society of Chemistry

The low molecular weight and high surface charge of C_{13}-KR offered a fast interfacial adsorption rate (400 Hz). Besides, the enhanced surface activity due to the good interfacial anchoring of the hydrocarbon chain decreased droplet size of the emulsion, with further size reduction achieved by either increasing the peptide concentration or prolongation of sonication time. Formation of stable highly elastic films at the interface in addition to the good surface activity enhanced storage stability. In addition, the high zeta potential of the C_{13}-KR stabilized droplets, conferring resistance to salting out and thermal aggregation.

Another lipopeptide emulsifier and gelator was formed via Schiff's base formation upon mixing the precursors A, hydrophilic peptide NH_2-lauroylGGGH, and B, lipophilic 1,4-phthalaldehyde, at ambient temperature with molar ratio of A:B 2:1 (Table 13.2) (Nishida et al. 2017). The product was a mixture of ABA and AB that self-assembled into nanofibres (30–100 nm) entangled into thicker bundles at pH 7.4 without heating. Entangled nanofibres stabilized emulsions in biphasic media and formed hydrogel in aqueous medium within short period, 1 and 15 min, respectively. The hydrogel storage modulus was higher than its loss modulus after 3 min of precursors blending and progressively increased by time confirming the self-assembly and gelation process. Gel–sol transition occurred by heating to 75 °C or changing the pH to low or high values due to protonation or hydrolysis of the Schiff's base. Fabrication of emulsion was triggered by homogenizing 4 parts by volume of aqueous phase containing A with 1 part of organic phase containing B with the amount of precursor A was double B quantity. Homogenization for 1 min yielded thinner nanofibril bundles of ABA and AB (30–40 nm thickness) at the interface only, to produce globules of 22.4 μm diameter, without gelation in the bulk phase. This system was not formed upon the use of single precursor only and this was confirmed by confocal laser scanning microscopy. Acidification of the system with HCl or heating to 80 °C led to disassembly of the interfacial nanofibres and droplets fusion into larger size. The formed emulsion droplets were employed as stimuli-sensitive microreactors to regulate a click reaction of an alkyne with an azide by entrapping each reactant in separate oil droplets of the emulsion stabilized by the nanofibres and then initiating the reaction on demand when disassembly induced by external stimulus (heating or acidification).

13.3 Protein Emulsifiers

Proteins have been widely used as emulsifying and foaming agent in food industry (Wilde et al. 2004; McClements 2004). They are readily available, natural and non-toxic; moreover, they can produce and stabilize emulsions with desirable physicochemical properties. Proteins adsorb to the interface and allow droplet dispersion through reduction of interfacial tension while hindering droplet coalescence via either steric stabilization or electrostatic repulsion of the formed protective layer (Fig. 13.9) (McClements 2004; Walstra 2003). In this section, we will expand

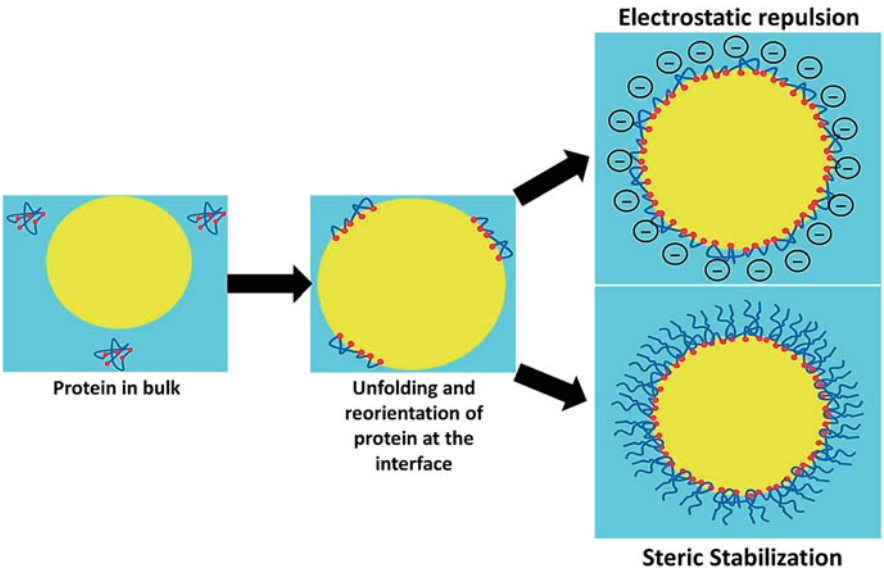

Fig. 13.9 The possible emulsion stabilization mechanisms using proteins by electrostatic repulsion or steric stabilization

more on the main protein emulsifiers, which have been commonly used in industry, such as milk proteins, hydrophobins, gelatin and pea proteins.

13.3.1 Milk Protein Emulsifiers

Milk proteins are mainly divided into two families, caseins and whey proteins.

13.3.1.1 Caseins

Caseins, belonging to phosphoproteins, are known to be the principal protein constituents in milk (80%) (Tomadoni et al. 2020). Caseins include four major flexible proteins, namely, α_{s1}-, α_{s2}-, β- and κ-casein. They are unstructured negatively charged proteins that do not form α-helices or β-sheets due to the numerous P residues in their sequence as well as absence of disulphide bonds (Bouyer et al. 2012; Tomadoni et al. 2020; Sarkar and Singh 2016). Caseins acquire self-assembled micellar forms upon binding to calcium phosphate in milk that interconnect via non-covalent bindings (Dickinson 2006). α_{s1} and β caseins are highly efficient emulsifiers that have good tendency to adsorb at oil/water interface and reduce interfacial tension as a result of their amphiphilicity (Table 13.3) (Bouyer

Table 13.3 Classification of the protein emulsifiers and their uses

Name of protein	Use	References
α_{s1} and β caseins	O/W emulsion	Bouyer et al. (2012)
Whey proteins (-β-lactoglobulin, α-lactalbumin and lactoferrin)	Food emulsions	Sedaghat Doost et al. (2019), Teo et al. (2016), Ng et al. (2017), Zhu et al. (2018), Fioramonti et al. (2015)
Hydrophobins	Foams and O/W emulsions	Paukkonen et al. (2017), Tchuenbou-Magaia et al. (2009), Green et al. (2013), Cox et al. (2007), Cox et al. (2009)
Gelatin	O/W emulsion Foam	Surh et al. (2006), Zarai et al. (2016)
Pea proteins (vicilin and legumin)	Emulsion	Burger and Zhang (2019), Liang and Tang (2014), Ducel et al. (2004), Sridharan et al. (2020)

et al. 2012). β-casein exhibited tail-like anchoring behaviour to the interface via its terminal part, while α_{s1} casein attached to the interface in a loop-like orientation through the mid-part of its sequence (Fig. 13.10).

β-casein showed better emulsification properties, more reduction of interfacial tension and higher preferential interfacial adsorption with thicker film formation than α_{s1} (Sarkar and Singh 2016). β-casein can also prevent the coalescence of globules for long time via two mechanisms: firstly steric as well as electrostatic repulsive forces through extended saturated monolayer film of 10 nm width as reported by Dickinson and Davies (1999) as well as Fang and Dalgleish (1998) and secondly the viscoelastic behaviour of the adsorbed protein film at the interface as illustrated by Bantchev and Schwartz (2003) and Gau et al. (1994) (Fig. 13.9). Despite its prominent surface activity, casein-based emulsions can easily flocculate when treated with calcium ions, due to screening of the protein's negative charge and thinning of its interfacial film (Dalgleish 1997; Agboola and Dalgleish 1995).

Sodium caseinate is the commonly used form as emulsifier which is the sodium salt of mixture of all casein proteins, as it is not possible to use individual types of casein because of the high purification cost of individual components (Bouyer et al. 2012; Sarkar and Singh 2016). Sodium caseinate is produced by reducing the pH of skimmed milk to 4.6 to precipitate the casein followed by solubilization using sodium salts at neutral pH and finally drying. Stabilization of the sodium caseinate-based O/W emulsions is affected by protein concentration, molecular orientation in the bulk phase and the components of protein interfacial film (Sarkar and Singh 2016).

The enzymatic hydrolysis of β-casein yielded 2 peptide sequences: a hydrophilic peptide (β-CN, f1–25) of 25 amino acids and a hydrophobic one (β-CN, f193–209) of 17 amino acids (Lee et al. 1987). These peptides showed poor emulsification properties at neutral pH, which was ascribed to the short length of these hydrolysates. However, surface activity improved at extreme pH (below 4 and above 8) in

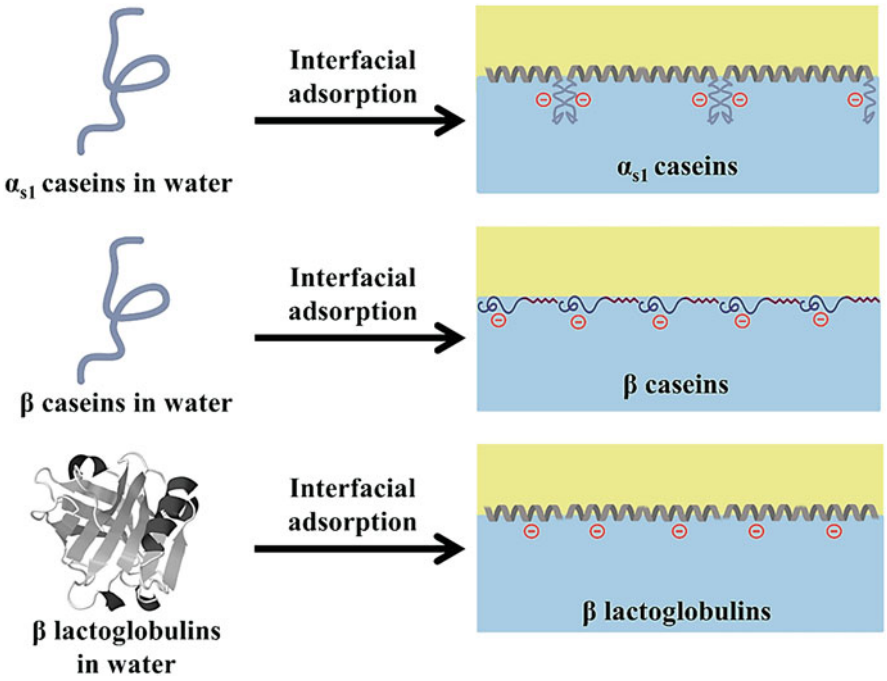

Fig. 13.10 Milk proteins interfacial adsorption where α_{s1} and β caseins acquire random coil structure in solution that adsorb to the emulsion interface and then β caseins exhibit tail-like anchoring behaviour to the interface via its terminal part, while α_{s1} casein attached to the interface in a loop-like orientation through the mid-part of its sequence. Moreover, the folded structure of β-lactoglobulin in water shows interconnected antiparallel β-sheets and flanked α-helices that rearranges upon adsorption to the interface. Adapted from (Dickinson 1998), with copyrights permission from Royal Society of Chemistry and (Zhai et al. 2011), reference with copyrights permission from the American Society of Chemistry

case of the β-CN, f193–209 sequence and at acidic pH for β-CN, f1–25 peptide. These casein-derived peptides showed formation of thick films around the oil droplets suggesting the possible association of peptides at the interface.

13.3.1.2 Whey Proteins

Milk whey proteins are primarily composed of 80% β-lactoglobulin and 15% α-lactalbumin with minor proteins of lactoferrin, serum albumin and immunoglobulins (Bouyer et al. 2012; Tomadoni et al. 2020). Unlike caseins, they have secondary, tertiary and quaternary structures connected by disulphide bridges, therefore not as flexible as casein (Bouyer et al. 2012). β-lactoglobulin and α-lactalbumin hold ideal emulsification characteristics and were utilized successfully to stabilize food emulsions; however, both possessed a slight lower stability than casein-based

emulsion in similar environment (Tcholakova et al. 2006; Dickinson 1997; Hunt and Dalgleish 1994; Dalgleish 1995). β-lactoglobulin, a dense folded protein, is constituted of 162 amino acid sequence containing 2 disulphide bridges as well as 1 free thiol moiety. Its folded structure shows interconnected antiparallel β-sheets and flanked α-helices (Fig. 13.10) (Sarkar and Singh 2016). After interfacial adsorption, partial unfolding is initiated with intermolecular binding of β-sheets through their free sulfhydryl groups to form disulphide bridges between molecules and develops a compact interfacial layer of 2 nm width irreversibly fortified upon storage with the increment of polymerization degree (Dickinson 1998; Dalgleish 2004). β-lactoglobulin is able to stabilize emulsions at neutral medium due to the protein negative charge that promoted electrostatic repulsion between emulsion globules besides reduction of interfacial tension (Kim et al. 2002; Wüstneck et al. 1999; Paulsson and Dejmek 1992). However, like most proteins, β-lactoglobulin is thermolabile, where it unfolds at 70 °C, resulting in protein aggregation and droplet coalescence (Kim et al. 2002; Ye 2010).

The second abundant whey protein, α-lactalbumin, is a calcium metalloprotein held together via 4 intrachain disulphide bridges without free thiol groups, unlike β-lactoglobulin (Sarkar and Singh 2016). α-lactalbumin possesses more C residues and less P moieties than β-lactoglobulin (Ng-Kwai-Hang 2003). In addition, α-lactalbumin thermally degrades at lower temperature (66 °C) than β-lactoglobulin without aggregation due to the absence of free thiols (Sarkar and Singh 2016; Considine et al. 2007). Dickinson et al. studied the competitive interfacial adsorption between both proteins and suggested the irreversible adsorption of the firstly added protein, which predominated the interface and could not be displaced by the secondly added one (Dickinson et al. 1989).

Lactoferrin is another whey protein component present in a minor level, composed of 700 amino acids capable of binding to iron and exhibits a high positive zeta potential (+50 mV) at neutral pH. It can therefore form stable emulsions of cationic droplets at a wider pH range (3–7), unlike caseinates and β-lactoglobulin that can stabilize emulsion at neutral pH only where their pI ranged between 4.5 and 5.5 (Baker and Baker 2005; Ye and Singh 2006). Wahlgren et al. reported the possibility of electrostatic attraction between the anionic β-lactoglobulin and the cationic lactoferrin (Wahlgren et al. 1993). Based on this, Ye and Singh developed stable O/W emulsions with thick films of multilayered binary protein mixture at neutral pH (Ye and Singh 2007). Although the net charge of the protein mixture is zero, the dense multilayers offered robust steric hindrance that prevented coalescence of the emulsion droplets.

The marketed forms of whey protein emulsifiers are whey protein concentrate (WPCs) (25–80% protein) and whey protein isolate (WPIs) (>90% protein) extensively utilized in food industries (Sarkar and Singh 2016). WPI has been also utilized to develop O/W emulsions using simple stirring methods (Table 13.3) (Sedaghat Doost et al. 2019; Teo et al. 2016; Ng et al. 2017; Zhu et al. 2018; Fioramonti et al. 2015).

To summarize, milk proteins are considered the most widely used bioemulsifier in food industry being a natural amphiphile, generally regarded as safe (GRAS),

i.e. biocompatible, non-toxic, biodegradable, offer great nutritional value and have antioxidant properties and easily sourced from milk, hence sustainable (Ha and Lee 2020; He et al. 2011). However, they suffer from batch-to-batch variabilities and immunogenicity where cow's milk is one of the eight main food categories causing 90% of food allergies (Nutten et al. 2020; Broersen 2020).

13.3.2 Hydrophobins

Hydrophobins are a group of globular fungal proteins that are believed to behave like small molecule emulsifiers. As a result of their high amphiphilicity, as well as rapid interfacial adsorption due to their relatively small sizes, hydrophobins showed the greatest surface activity between all types of protein emulsifiers (Paukkonen et al. 2017; Berger and Sallada 2019). They can be classified according to their self-assembled conformation, hydropathy patterns and solubility into two types: class I as SC3 that yields insoluble rodlets with amyloid orientation solely soluble in strong acids, and class II, like HFBI and HFBII, which acquire highly organized 2D interfacial monolayers. Class II also are widely soluble in organic solvents and detergents and easily solubilized in water even at high concentration (100 mg/mL) (Paukkonen et al. 2017; Berger and Sallada 2019). Hydrophobins possess 4 disulphide bridges in their tertiary structure and show intermolecular interactions which allow self-association as amphipathic elastic monolayer films at oil/water and air/water interfaces. Hence, they decrease interfacial tension and can change the behaviour of surfaces from lipophilic nature to hydrophilic and vice versa (Paukkonen et al. 2017; Paananen et al. 2013). Therefore, hydrophobins are suitable for formulation of foams and O/W emulsions with long-term stability up to 4 months at ambient storage conditions (Table 13.3) (Paukkonen et al. 2017; Tchuenbou-Magaia et al. 2009; Green et al. 2013; Cox et al. 2007, 2009) and are considered as non-toxic and non-immunogenic pharmaceutical excipients (Aimanianda et al. 2009; Ebbole 1997).

13.3.3 Gelatin

Gelatin is a high-molecular weight protein obtained by hydrolysis of animal collagen via boiling at acidic pH to yield Type A gelatin or basic pH to produce Type B gelatin (Bouyer et al. 2012; Taherian et al. 2011). The difference in their preparation method led to differences in their physicochemical properties where pI of Type A gelation is ranged from 7 to 9, whereas Type B gelatin is 4.8 to 5.1 (Djagny et al. 2001). Such variation in characteristic was attributed to that basic hydrolysis of collagen had converted N and Q into D and E that yielded Type B gelatin (Veis 1964).

Gelatin proteins showed to have some surface activity. Both low- and high-molecular weight fish gelatin demonstrated to stabilize 20% corn oil in water as O/W emulsion at ≥4% w/w total gelatin concentration as reported by Surh and co-workers (Table 13.3) (Surh et al. 2006). However, large oil droplets (>10 μm) were observed in the emulsion due to low surface activity of gelatin, which could lead to coalescence. Low-molecular weight fish gelatin produced greater fractions of large droplets than high-molecular weight one; however, emulsions formed by the earlier were more stable against creaming. Emulsions stabilized by fish gelatin showed resistance to phase separation at pH range between 3 and 8, heating for 30 min at 90 °C and NaCl salt up to 250 mM.

Land snails-derived gelatin also possessed interfacial activity. Zarai et al. studied the emulsifying properties of this gelatin and suggested the possibility to act a bioemulsifier, since it demonstrated to stabilize olive O/W emulsions at total gelatin concentrations of 0.5–4% w/v (Table 13.3) (Zarai et al. 2016). At high gelatin levels, a crosslinked 3D matrix was formed in the bulk phase, which, in addition to its interfacial adsorption, help trapping the oil globules inside the hydrogel network forming a strong emulgel. Land snails-derived gelatin produced emulsions with higher stability than other gelatins from different origins (smooth hound, zebra blenny, barbel and grey triggerfish), could be attributed to the differences in composition, protein conformation and properties. Snail gelatin also produced dense stable foams at high concentrations 1–4%w/v due to the formation of interfacial thick gelatin films, but markedly collapsed after 1 hour of mixing (Zarai et al. 2016).

13.3.4 Pea Proteins

Pea proteins include two main constituents: vicilin, a 7S storage globulin, and legumin, a 11S storage globulin (Gueguen et al. 1988). Legumin protein consists of linked subunits via non-covalent binding in a hexameric structure, while vicilin protein shows a trimeric conformation (Bouyer et al. 2012; Burger and Zhang 2019). The ratio between legumin and vicilin, as well as their structures, differs depending on the production technique and species, consequently variation of their functions. In general, vicilin possessed higher surface activity and emulsion stabilization efficiency than legumin (Burger and Zhang 2019). Pea proteins successfully produced emulsions through interfacial adsorption that occurred in two stages. Firstly, protein migration from aqueous phase and anchoring to the oil/water interface via the exposed hydrophobic part of the molecule. Secondly, protein reorientation occurred to position the hydrophilic parts towards the aqueous phase and solubilize the lipophilic areas in the organic phase forming a viscoelastic rigid interfacial layer that stabilized the system by steric effect and electrostatic repulsions (Burger and Zhang 2019; Sridharan et al. 2020). In essence, pea proteins are capable of reducing interfacial tension (Ducel et al. 2004) and stabilize emulsion formation at low pH both by Pickering mechanism and hydrogelation (Table 13.3) (Liang and Tang 2014). However, pea proteins emulsions could not withstand changing salts

concentration, where increasing NaCl concentration of 50 to 200 mM enlarged the emulsion droplet from 6 to 14.05 μm and the medium pH should be away from its pI (4.5) where the extreme pH values (pH 3 and 8) were preferred to allow the charging of protein molecules, so it was necessary to add another emulsifier, such as pectin, to stabilize emulsions and prevent phase separation in harsh conditions (Gharsallaoui et al. 2010a, b; Ettoumi et al. 2016; Ladjal-Ettoumi et al. 2016).

13.4 Protein–Polysaccharide Mixed Emulsifiers

On one hand, proteins are characterized by the quick interfacial adsorption and film formation that prohibits emulsion coalescence, though stability can always be impaired either by changing pH near to pI or by salting out (Ozturk and McClements 2016; Yang et al. 2019). On the other hand, polysaccharides can develop highly stable emulsions but using extremely high polymer levels (Chen et al. 2011b; Kharat et al. 2018). Therefore, combining both proteins and polysaccharides via covalent conjugation, electrostatic attractions or by physical mixing combines the attributes of both components, fast interfacial adsorption of protein in addition to the viscosity increment and steric hindrance of polysaccharides, thus creating highly stable emulsions (de Oliveira et al. 2016; Setiowati et al. 2020). In this section we will discuss protein–polysaccharide mixed emulsifiers formed by covalent conjugation and non-covalent interaction.

13.4.1 Protein–Polysaccharide Covalent Conjugates

Controlled Maillard reaction was used to conjugate amino groups of protein with the carbonyl functionalities of polysaccharides to yield composites having higher emulsifying power than either polysaccharides or proteins alone, such as sodium caseinate/maltodextrin (O'Regan and Mulvihill 2010), β-lactoglobulin/dextran (Wooster and Augustin 2006) and whey protein isolate/maltodextrin (Akhtar and Dickinson 2007). These complexes also offered resistance to undesirable environmental conditions, such as freezing, heating or great ionic strength (Bouyer et al. 2012; Setiowati et al. 2020). For instance, O'Regan and Mulvihill previously showed the augmented stability of emulsion formulated using sodium caseinate maltodextrin for 7 days at 45 °C in comparison to sodium caseinate (O'Regan and Mulvihill 2010). Setiowati and co-workers also demonstrated that chemical conjugation of whey protein isolate to low methoxy pectin resulted in a conjugate of superior interfacial activity and emulsion stabilization than the electrostatic complex (Diah Setiowati et al. 2019; Setiowati et al. 2017).

Zhang et al. showed the effect of glycosylation of soy protein isolates with maltodextrin using Maillard reaction on the emulsification of fish oil compared with soy protein isolate/maltodextrin mixture where smaller droplet size, lower

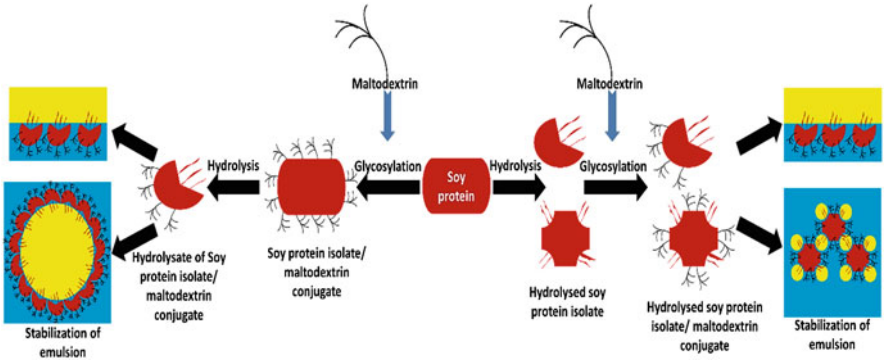

Fig. 13.11 O/W emulsion stabilization through conjugation between the hydrolysed soy protein and maltodextrin or hydrolysis of the conjugated soy protein and maltodextrin using Maillard reaction. Adapted from (Zhang et al. 2015), and (Zhang et al. 2014), with copyrights permission from Elsevier

polydispersity index and improved physical stability (3-week storage) were observed with both hydrolysate of soy protein isolate/maltodextrin conjugate and hydrolysed soy protein isolate/maltodextrin conjugate-based O/W emulsions (Fig. 13.11) (Zhang et al. 2014, 2015).

13.4.2 Protein–Polysaccharide Physical Mixtures

Electrostatic interactions between counter charge polysaccharides and proteins at the interface were claimed to boost the emulsion stability (Li et al. 2019). There are two main reported methods for mixing emulsifiers, where one method involved one pot mixing of the two components to prepare the complex necessary for emulsion production (Yang et al. 2019; Lutz et al. 2009; Laplante et al. 2006; Yildiz et al. 2018). However, the other method is layer by layer electrostatic deposition, where initially a primary protein-based emulsion was developed followed by incorporating the polysaccharide to the system that interacted at droplet interface with the protein to form a second coat around droplets (Khalloufi et al. 2009). These deposition steps could be repeated several times to produce multicoats stabilizing the emulsion.

Initial emulsification with protein is essential, as protein emulsifiers exhibit fast stabilization kinetics and reduction of interfacial tension. The protein–polysaccharide mixed emulsifiers showed greater resistance to environmental conditions including dehydration, high salt concentrations and temperature changes. For example, coalescence of casein-based emulsion near the pI of casein was substantially hindered by adding octenyl succinic anhydride modified starch (OSAS) and this blend demonstrated higher oxidative stability than OSAS-based emulsion (Yang et al. 2019).

Another physical mixing approach, not involving electrostatic interaction, depends on addition of a protein emulsifier to the biphasic system for interfacial adsorption and formation of small globules of the internal phase. This is followed by the introduction of the polysaccharide component as a viscosity modifying agent, which enhances the viscosity of the continuous aqueous phase via thickened networks and hampers droplet movement, thus preventing creaming/sedimentation of the internal phase droplets. Several mixtures were prepared by the viscosity enhancement method, such as whey protein isolate/xanthan gum (Sun and Gunasekaran 2009), sodium caseinate/locust bean gum (Perrechil and Cunha 2010), sodium caseinate/xanthan gum (Moschakis et al. 2005) and whey protein isolate/flaxseed gum (Khalloufi et al. 2008).

13.5 Summary

Short peptides are emerging new class of bioemulsifiers that have been shown to stabilize different foams and emulsions and have proven to be superior to traditional commercial emulsifiers in long-term stabilization of these colloidal systems. Besides, peptides are similar to proteins in being safe, biodegradable, biocompatible and of low toxicity to human health and environment, thus overcoming the common limitations of the currently used traditional emulsifiers. On the top of these, the physicochemical properties of peptide emulsifiers can be finely tuned by the rational chemical design of the amino acid sequence, providing a plethora of design options for controlling their behaviour at the organic/aqueous and gas/aqueous interfaces. In general, peptide-based emulsification was reported to occur either via micelle-like structure formation, akin to conventional emulsifier, or through self-assembly into amphiphilic nanofibrous structure at the interface and in bulk continuous phase. Proteins have also been widely used in food industry to stabilize emulsions, through steric stabilization and/or electrostatic repulsion. However, proteins have some limitations, mainly due to the possible batch-to-batch variation, chemical and physical instability as well as potential immunogenicity. Protein–polysaccharide mixed emulsifiers have also been introduced but have shown to be less efficient in stabilizing emulsions and foams when compared to peptides and proteins. In brief, peptides and proteins are important emerging subclasses of bioemulsifier armamentarium, though there is still a lot of work to be done for their wide utilization in industry, when it comes to large-scale production of these molecules, as well as tackling stability issues during storage and manufacturing.

Acknowledgments Newton-Mosharafa fund awarded to A.K. and M.A.E. and Egyptian Government mission's sector PhD scholarship to M.S.

References

Adjonu R, Doran G, Torley P, Agboola S (2014) Whey protein peptides as components of nanoemulsions: a review of emulsifying and biological functionalities. J Food Eng 122:15–27

Agboola SO, Dalgleish DG (1995) Calcium-induced destabilization of oil-in-water emulsions stabilized by caseinate or by β-lactoglobulin. J Food Sci 60:399–404

Aggeli A, Nyrkova IA, Bell M, Harding R, Carrick L, McLeish TC, Semenov AN, Boden N (2001) Hierarchical self-assembly of chiral rod-like molecules as a model for peptide β-sheet tapes, ribbons, fibrils, and fibers. Proc Natl Acad Sci 98:11857–11862

Aimanianda V, Bayry J, Bozza S, Kniemeyer O, Perruccio K, Elluru SR, Clavaud C, Paris S, Brakhage AA, Kaveri SV (2009) Surface hydrophobin prevents immune recognition of airborne fungal spores. Nature 460:1117–1121

Akhtar M, Dickinson E (2007) Whey protein-maltodextrin conjugates as emulsifying agents: an alternative to gum Arabic. Food Hydrocoll 21:607–616

Aviño F, Matheson AB, Adams DJ, Clegg PS (2017) Stabilizing bubble and droplet interfaces using dipeptide hydrogels. Org Biomol Chem 15:6342–6348

Bai S, Pappas C, Debnath S, Frederix PW, Leckie J, Fleming S, Ulijn RV (2014) Stable emulsions formed by self-assembly of interfacial networks of dipeptide derivatives. ACS Nano 8:7005–7013

Baker EN, Baker HM (2005) Lactoferrin. Cell Mol Life Sci 62:2531

Bantchev GB, Schwartz DK (2003) Surface shear rheology of β-casein layers at the air/solution interface: formation of a two-dimensional physical gel. Langmuir 19:2673–2682

Berger BW, Sallada ND (2019) Hydrophobins: multifunctional biosurfactants for interface engineering. J Biol Eng 13:10

Besseling N (1997) Theory of hydration forces between surfaces. Langmuir 13:2113–2122

Bouyer E, Mekhloufi G, Rosilio V, Grossiord J, Agnely F (2012) Proteins, polysaccharides, and their complexes used as stabilizers for emulsions: alternatives to synthetic surfactants in the pharmaceutical field? Int J Pharm 436:359–378

Broersen K (2020) Milk processing affects structure, bioavailability and immunogenicity of β-lactoglobulin. Foods 9:874

Burger TG, Zhang Y (2019) Recent progress in the utilization of pea protein as an emulsifier for food applications. Trends Food Sci Technol 86:25

Caballero B, Trugo LC, Finglas PM (2003) Encyclopedia of food sciences and nutrition, 2nd edn. Academic

Callender SP, Mathews JA, Kobernyk K, Wettig SD (2017) Microemulsion utility in pharmaceuticals: implications for multi-drug delivery. Int J Pharm 526:425–442

Castelletto V, Edwards-Gayle CJ, Hamley IW, Barrett G, Seitsonen J, Ruokolainen J (2019) Peptide-stabilized emulsions and gels from an arginine-rich surfactant-like peptide with antimicrobial activity. ACS Appl Mater Interfaces 11:9893–9903

Chen L, Pont G, Morris K, Lotze G, Squires A, Serpell LC, Adams DJ (2011a) Salt-induced hydrogelation of functionalised-dipeptides at high pH. Chem Commun 47:12071–12073

Chen B, Li H, Ding Y, Rao J (2011b) Improvement of physicochemical stabilities of emulsions containing oil droplets coated by non-globular protein-beet pectin complex membranes. Food Res Int 44:1468–1475

Considine T, Patel HA, Anema SG, Singh H, Creamer LK (2007) Interactions of milk proteins during heat and high hydrostatic pressure treatments-a review. Innovative Food Sci Emerg Technol 8:1–23

Cox AR, Cagnol F, Russell AB, Izzard MJ (2007) Surface properties of class II hydrophobins from Trichoderma reesei and influence on bubble stability. Langmuir 23:7995–8002

Cox AR, Aldred DL, Russell AB (2009) Exceptional stability of food foams using class II hydrophobin HFBII. Food Hydrocoll 23:366–376

Dalgleish D (1995) Structures and properties of adsorbed layers in emulsions containing milk proteins. In: Structures and properties of adsorbed layers in emulsions containing milk proteins. Food Macromolecules and Colloids, pp 23–33

Dalgleish DG (1997) Adsorption of protein and the stability of emulsions. Trends Food Sci Technol 8:1–6

Dalgleish DG (2004) Food emulsions: their structures and properties. Food Emulsions 4

de Oliveira FC, Coimbra JS, dos Reis EB, de Oliveira ADG, Zuñiga EEGR (2016) Food protein-polysaccharide conjugates obtained via the Maillard reaction: a review. Crit Rev Food Sci Nutr 56:1108–1125

Dexter AF (2010) Interfacial and emulsifying properties of designed β-strand peptides. Langmuir 26:17997–18007

Dexter AF, Middelberg AP (2007) Switchable peptide surfactants with designed metal binding capacity. J Phys Chem C 111:10484–10492

Dexter AF, Malcolm AS, Middelberg AP (2006) Reversible active switching of the mechanical properties of a peptide film at a fluid–fluid interface. Nat Mater 5:502–506

Diah Setiowati A, Rwigamba A, Van der Meeren P (2019) The influence of degree of methoxylation on the emulsifying and heat stabilizing activity of whey protein-pectin conjugates. Food Hydrocoll 96:54–64

Dickinson E (1997) Properties of emulsions stabilized with milk proteins: overview of some recent developments. J Dairy Sci 80:2607–2619

Dickinson E (1998) Proteins at interfaces and in emulsions stability, rheology and interactions. J Chem Soc Faraday Trans 94:1657–1669

Dickinson E (2006) Colloid science of mixed ingredients. Soft Matter 2:642–652

Dickinson E, Davies E (1999) Influence of ionic calcium on stability of sodium caseinate emulsions. Colloids Surf B: Biointerfaces 12:203–212

Dickinson E, Rolfe SE, Dalgleish DG (1989) Competitive adsorption in oil-in-water emulsions containing α-lactalbumin and β-lactoglobulin. Food Hydrocoll 3:193–203

Djagny KB, Wang Z, Xu S (2001) Gelatin: a valuable protein for food and pharmaceutical industries. Crit Rev Food Sci Nutr 41:481–492

Dragulska SA, Chen Y, Wlodarczyk MT, Poursharifi M, Dottino P, Ulijn RV, Martignetti JA, Mieszawska AJ (2018) Tripeptide-stabilized oil-in-water nanoemulsion of an oleic acids–Platinum (II) conjugate as an anticancer nanomedicine. Bioconjug Chem 29:2514–2519

Ducel V, Richard J, Popineau Y, Boury F (2004) Adsorption kinetics and rheological interfacial properties of plant proteins at the oil-water Interface. Biomacromolecules 5:2088–2093

Dwyer MD, He L, James M, Nelson A, Middelberg AP (2013) Insights into the role of protein molecule size and structure on interfacial properties using designed sequences. J R Soc Interface 10:20120987

Ebbole DJ (1997) Hydrophobins and fungal infection of plants and animals. Trends Microbiol 5: 405–408

Ettoumi YL, Chibane M, Romero A (2016) Emulsifying properties of legume proteins at acidic conditions: effect of protein concentration and ionic strength, LWT-food. Sci Technol 66:260–266

Fang Y, Dalgleish DG (1998) The conformation of α-lactalbumin as a function of pH, heat treatment and adsorption at hydrophobic surfaces studied by FTIR. Food Hydrocoll 12:121–126

Fioramonti SA, Arzeni C, Pilosof AMR, Rubiolo AC, Santiago LG (2015) Influence of freezing temperature and maltodextrin concentration on stability of linseed oil-in-water multilayer emulsions. J Food Eng 156:31–38

Fowler CI, Muchemu CM, Miller RE, Phan L, O'Neill C, Jessop PG, Cunningham MF (2011) Emulsion polymerization of styrene and methyl methacrylate using cationic switchable surfactants. Macromolecules 44:2501–2509

Gao B, Wyttenbach T, Bowers MT (2009) Protonated arginine and protonated lysine: hydration and its effect on the stability of salt-bridge structures. J Phys Chem B 113:9995–10000

Garcia AM, Kurbasic M, Kralj S, Melchionna M, Marchesan S (2017) A biocatalytic and thermoreversible hydrogel from a histidine-containing tripeptide. Chem Commun 53:8110–8113

Gau CS, Yu H, Zografi G (1994) Surface viscoelasticity of β-casein monolayers at the air/water interface by electrocapillary wave diffraction. J Colloid Interface Sci 162:214–221

Gazit E (2007) Self assembly of short aromatic peptides into amyloid fibrils and related nanostructures. Prion 1:32–35

Gharsallaoui A, Saurel R, Chambin O, Cases E, Voilley A, Cayot P (2010a) Utilisation of pectin coating to enhance spray-dry stability of pea protein-stabilised oil-in-water emulsions. Food Chem 122:447–454

Gharsallaoui A, Yamauchi K, Chambin O, Cases E, Saurel R (2010b) Effect of high methoxyl pectin on pea protein in aqueous solution and at oil/water interface. Carbohydr Polym 80:817–827

Green AJ, Littlejohn KA, Hooley P, Cox PW (2013) Formation and stability of food foams and aerated emulsions: hydrophobins as novel functional ingredients. Curr Opin Colloid Interface Sci 18:292–301

Gueguen J, Chevalier M, And JB, Schaeffer F (1988) Dissociation and aggregation of pea legumin induced by pH and ionic strength. J Sci Food Agric 44:167–182

Guler MO, Stupp SI (2007) A self-assembled nanofiber catalyst for ester hydrolysis. J Am Chem Soc 129:12082–12083

Ha H, Lee W (2020) Milk protein-stabilized emulsion delivery system and its application to foods. J Dairy Sci Biotechnol 38:189–196

Hanson JA, Chang CB, Graves SM, Li Z, Mason TG, Deming TJ (2008) Nanoscale double emulsions stabilized by single-component block copolypeptides. Nature 455:85–88

He W, Tan Y, Tian Z, Chen L, Hu F, Wu W (2011) Food protein-stabilized nanoemulsions as potential delivery systems for poorly water-soluble drugs: preparation, in vitro characterization, and pharmacokinetics in rats. Int J Nanomedicine 6:521

Huang Z, Guan S, Wang Y, Shi G, Cao L, Gao Y, Dong Z, Xu J, Luo Q, Liu J (2013) Self-assembly of amphiphilic peptides into bio-functionalized nanotubes: a novel hydrolase model. J Mater Chem B 1:2297–2304

Hui Y, Wibowo D, Zhao C (2016) Insights into the role of biomineralizing peptide surfactants on making nanoemulsion-templated silica nanocapsules. Langmuir 32:822–830

Hunt JA, Dalgleish DG (1994) Adsorption behaviour of whey protein isolate and caseinate in soya oil-in-water emulsions. Food Hydrocoll 8:175–187

Khalloufi S, Alexander M, Goff HD, Corredig M (2008) Physicochemical properties of whey protein isolate stabilized oil-in-water emulsions when mixed with flaxseed gum at neutral pH. Food Res Int 41:964–972

Khalloufi S, Corredig M, Goff HD, Alexander M (2009) Flaxseed gums and their adsorption on whey protein-stabilized oil-in-water emulsions. Food Hydrocoll 23:611–618

Kharat M, Zhang G, McClements DJ (2018) Stability of curcumin in oil-in-water emulsions: impact of emulsifier type and concentration on chemical degradation. Food Res Int 111:178–186

Kim H, Decker EA, McClements DJ (2002) Role of postadsorption conformation changes of β-lactoglobulin on its ability to stabilize oil droplets against flocculation during heating at neutral pH. Langmuir 18:7577–7583

Ladjal-Ettoumi Y, Boudries H, Chibane M, Romero A (2016) Pea, chickpea and lentil protein isolates: physicochemical characterization and emulsifying properties. Food Biophysics 11:43–51

Laplante S, Turgeon SL, Paquin P (2006) Emulsion-stabilizing properties of chitosan in the presence of whey protein isolate: effect of the mixture ratio, ionic strength and pH. Carbohydr Polym 65:479–487

Lee YS (2008) Self-assembly and nanotechnology: a force balance approach. Wiley

Lee SW, Shimizu M, Kaminogawa S, Yamauchi K (1987) Emulsifying properties of peptides obtained from the hydrolyzates of β-casein. Agric Biol Chem 51:161–166

Li T, Kalloudis M, Cardoso AZ, Adams DJ, Clegg PS (2014) Drop-casting hydrogels at a liquid interface: the case of hydrophobic dipeptides. Langmuir 30:13854–13860
Li T, Nudelman F, Tavacoli JW, Vass H, Adams DJ, Lips A, Clegg PS (2016) Long-lived foams stabilized by a hydrophobic dipeptide hydrogel. Adv Mater Interfaces 3:1500601
Li Q, Wang Z, Dai C, Wang Y, Chen W, Ju X, Yuan J, He R (2019) Physical stability and microstructure of rapeseed protein isolate/gum Arabic stabilized emulsions at alkaline pH. Food Hydrocoll 88:50–57
Liang H, Tang C (2014) Pea protein exhibits a novel Pickering stabilization for oil-in-water emulsions at pH 3.0, vol 58. LWT-Food Sci Technol, pp 463–469
Lotfallah AH, Burguete MI, Alfonso I, Luis SV (2015) Highly stable oil-in-water emulsions with a gemini amphiphilic pseudopeptide. RSC Adv 5:36890–36893
Lutz R, Aserin A, Wicker L, Garti N (2009) Double emulsions stabilized by a charged complex of modified pectin and whey protein isolate. Colloids Surf B: Biointerfaces 72:121–127
Lv W, Hu T, Taha A, Wang Z, Xu X, Pan S, Hu H (2019) Lipo-dipeptide as an emulsifier: performance and possible mechanism. J Agric Food Chem 67:6377–6386
McClements DJ (2004) Protein-stabilized emulsions. Curr Opin Colloid Interface Sci 9:305–313
McClements DJ (2012) Nanoemulsions versus microemulsions: terminology, differences, and similarities. Soft Matter 8:1719–1729
Middelberg AP, Dimitrijev-Dwyer M (2011) A designed biosurfactant protein for switchable foam control. ChemPhysChem 12:1426–1429
Middelberg AP, Radke CJ, Blanch HW (2000) Peptide interfacial adsorption is kinetically limited by the thermodynamic stability of self association. Proc Natl Acad Sci 97:5054–5059
Middelberg AP, He L, Dexter AF, Shen H, Holt SA, Thomas RK (2008) The interfacial structure and Young's modulus of peptide films having switchable mechanical properties. J R Soc Interface 5:47–54
Minkenberg CB, Florusse L, Eelkema R, Koper GJ, van Esch JH (2009) Triggered self-assembly of simple dynamic covalent surfactants. J Am Chem Soc 131:11274–11275
Mondal S, Adler-Abramovich L, Lampel A, Bram Y, Lipstman S, Gazit E (2015) Formation of functional super-helical assemblies by constrained single heptad repeat. Nat Commun 6:1–8
Mondal S, Varenik M, Bloch DN, Atsmon-Raz Y, Jacoby G, Adler-Abramovich L, Shimon LJ, Beck R, Miller Y, Regev O, Gazit E (2017) A minimal length rigid helical peptide motif allows rational design of modular surfactants. Nat Commun 8:14018
Moreira IP, Sasselli IR, Cannon DA, Hughes M, Lamprou DA, Tuttle T, Ulijn RV (2016) Enzymatically activated emulsions stabilised by interfacial nanofibre networks. Soft Matter 12:2623–2631
Moreira IP, Piskorz TK, van Esch JH, Tuttle T, Ulijn RV (2017) Biocatalytic self-assembly of tripeptide gels and emulsions. Langmuir 33:4986–4995
Morikawa M, Yoshihara M, Endo T, Kimizuka N (2005) α-helical polypeptide microcapsules formed by emulsion-templated self-assembly. Chem–A Eur J 11:1574–1578
Moschakis T, Murray BS, Dickinson E (2005) Microstructural evolution of viscoelastic emulsions stabilised by sodium caseinate and xanthan gum. J Colloid Interface Sci 284:714–728
Myers D (1999) Surfaces, interfaces, and colloids, 2nd edn. Wiley, New York
Naseef MA, Ibrahim HK, Nour SAE (2018) Solid form of lipid-based self-nanoemulsifying drug delivery systems for minimization of diacerein adverse effects: development and bioequivalence evaluation in albino rabbits. AAPS PharmSciTech 19:3097–3109
Ng S, Nyam K, Lai O, Nehdi IA, Chong G, Tan C (2017) Development of a palm olein oil-in-water (o/w) emulsion stabilized by a whey protein isolate nanofibrils-alginate complex. LWT Food Sci Technol 82:311–317
Ng-Kwai-Hang KF (2003) Milk proteins heterogeneity. fractionation and isolation. Encyclopedia of Dairy Sciences 1881–1894
Nishida Y, Tanaka A, Yamamoto S, Tominaga Y, Kunikata N, Mizuhata M, Maruyama T (2017) In situ synthesis of a supramolecular hydrogelator at an oil/water Interface for stabilization and stimuli-induced fusion of microdroplets. Angew Chem 129:9538–9542

Nutten S, Schuh S, Dutter T, Heine RG, Kuslys M (2020) Design, quality, safety and efficacy of extensively hydrolyzed formula for management of cow's milk protein allergy: what are the challenges? Adv Food Nutr Res 93:147–204

O'Regan J, Mulvihill DM (2010) Sodium caseinate-maltodextrin conjugate stabilized double emulsions: encapsulation and stability. Food Res Int 43:224–231

Okochi H, Nakano M (2000) Preparation and evaluation of w/o/w type emulsions containing vancomycin. Adv Drug Deliv Rev 45:5–26

Ozturk B, McClements DJ (2016) Progress in natural emulsifiers for utilization in food emulsions, current opinion in food. Science 7:1–6

Paananen A, Ercili-Cura D, Saloheimo M, Lantto R, Linder MB (2013) Directing enzymatic cross-linking activity to the air-water interface by a fusion protein approach. Soft Matter 9:1612–1619

Parsons DF, Ninham BW (2010) Charge reversal of surfaces in divalent electrolytes: the role of ionic dispersion interactions. Langmuir 26:6430–6436

Paukkonen H, Ukkonen A, Szilvay G, Yliperttula M, Laaksonen T (2017) Hydrophobin-nanofibrillated cellulose stabilized emulsions for encapsulation and release of BCS class II drugs. Eur J Pharm Sci 100:238–248

Paulsson M, Dejmek P (1992) Surface film pressure of β-lactoglobulin, α-lactalbumin and bovine serum albumin at the air/water interface studied by Wilhelmy plate and drop volume. J Colloid Interface Sci 150:394–403

Perrechil FA, Cunha RL (2010) Oil-in-water emulsions stabilized by sodium caseinate: influence of pH, high-pressure homogenization and locust bean gum addition. J Food Eng 97:441–448

Petsev DN (2004) Emulsions: structure, stability and interactions. Elsevier

Platzman I, Janiesch J, Spatz JP (2013) Synthesis of nanostructured and biofunctionalized water-in-oil droplets as tools for homing T cells. J Am Chem Soc 135:3339–3342

Rapaport H, Kjaer K, Jensen TR, Leiserowitz L, Tirrell DA (2000) Two-dimensional order in β-sheet peptide monolayers. J Am Chem Soc 122:12523–12529

Rebello S, Asok AK, Mundayoor S, Jisha MS (2014) Surfactants: toxicity, remediation and green surfactants. Environ Chem Lett 12:275–287

Sarkar A, Singh H (2016) Emulsions and foams stabilised by milk proteins. In: Emulsions and foams stabilised by milk proteins. Advanced Dairy Chemistry, Springer, pp 133–153

Scott GG, McKnight PJ, Tuttle T, Ulijn RV (2016) Tripeptide emulsifiers. Adv Mater 28:1381–1386

Sedaghat Doost A, Nikbakht Nasrabadi M, Kassozi V, Dewettinck K, Stevens CV, Van der Meeren P (2019) Pickering stabilization of thymol through green emulsification using soluble fraction of almond gum – whey protein isolate nano-complexes. Food Hydrocoll 88:218–227

Setiowati AD, Saeedi S, Wijaya W, Van der Meeren P (2017) Improved heat stability of whey protein isolate stabilized emulsions via dry heat treatment of WPI and low methoxyl pectin: effect of pectin concentration, pH, and ionic strength. Food Hydrocoll 63:716–726

Setiowati AD, Wijaya W, Van der Meeren P (2020) Whey protein-polysaccharide conjugates obtained via dry heat treatment to improve the heat stability of whey protein stabilized emulsions. Trends Food Sci Technol 98:150

Sridharan S, Meinders MB, Bitter JH, Nikiforidis CV (2020) On the emulsifying properties of self-assembled pea protein particles. Langmuir 36:12221–12229

Sun C, Gunasekaran S (2009) Effects of protein concentration and oil-phase volume fraction on the stability and rheology of menhaden oil-in-water emulsions stabilized by whey protein isolate with xanthan gum. Food Hydrocoll 23:165–174

Surh J, Decker EA, McClements DJ (2006) Properties and stability of oil-in-water emulsions stabilized by fish gelatin. Food Hydrocoll 20:596–606

Taherian AR, Britten M, Sabik H, Fustier P (2011) Ability of whey protein isolate and/or fish gelatin to inhibit physical separation and lipid oxidation in fish oil-in-water beverage emulsion. Food Hydrocoll 25:868–878

Tavares FW, Bratko D, Blanch HW, Prausnitz JM (2004) Ion-specific effects in the colloid– colloid or protein– protein potential of mean force: role of salt– macroion van der Waals interactions. J Phys Chem B 108:9228–9235
Tcholakova S, Denkov ND, Ivanov IB, Campbell B (2006) Coalescence stability of emulsions containing globular milk proteins. Adv Colloid Interf Sci 123:259–293
Tchuenbou-Magaia FL, Norton IT, Cox PW (2009) Hydrophobins stabilised air-filled emulsions for the food industry. Food Hydrocoll 23:1877–1885
Teo A, Dimartino S, Lee SJ, Goh KKT, Wen J, Oey I, Ko S, Kwak H (2016) Interfacial structures of whey protein isolate (WPI) and lactoferrin on hydrophobic surfaces in a model system monitored by quartz crystal microbalance with dissipation (QCM-D) and their formation on nanoemulsions. Food Hydrocoll 56:150–160
Tian YF, Devgun JM, Collier JH (2011) Fibrillized peptide microgels for cell encapsulation and 3D cell culture. Soft Matter 7:6005–6011
Tomadoni B, Capello C, Valencia GA, Gutiérrez TJ (2020) Self-assembled proteins for food applications: a review. Trends Food Sci Technol 101:1
van Aken GA (2004) Coalescence mechanisms in protein-stabilized emulsions. Food Emulsions 299:325
Veis A (1964) The macromolecular chemistry of gelatin. Academic, New York
Wahlgren MC, Arnebrant T, Paulsson MA (1993) The adsorption from solutions of β-lactoglobulin mixed with lactoferrin or lysozyme onto silica and methylated silica surfaces. J Colloid Interface Sci 158:46–53
Walstra P (2003) Physical chemistry of foods. Marcel Decker, New York
Wang M, Lv Y, Liu X, Qi W, Su R, He Z (2016) Enhancing the activity of peptide-based artificial hydrolase with catalytic Ser/His/Asp triad and molecular imprinting. ACS Appl Mater Interfaces 8:14133–14141
Wang H, Wibowo D, Shao Z, Middelberg AP, Zhao C (2017) Design of modular peptide surfactants and their surface activity. Langmuir 33:7957–7967
Wibowo D, Zhao C, Middelberg AP (2014) Emulsion-templated silica nanocapsules formed using bio-inspired silicification. Chem Commun 50:11325–11328
Wibowo D, Wang H, Shao Z, Middelberg AP, Zhao C (2017) Interfacial films formed by a biosurfactant modularized with a silken tail. J Phys Chem C 121:14658–14667
Wilde PJ (2000) Interfaces: their role in foam and emulsion behaviour. Curr Opin Colloid Interface Sci 5:176–181
Wilde P, Mackie A, Husband F, Gunning P, Morris V (2004) Proteins and emulsifiers at liquid interfaces. Adv Colloid Interf Sci 108:63–71
Windbergs M, Zhao Y, Heyman J, Weitz DA (2013) Biodegradable core–shell carriers for simultaneous encapsulation of synergistic actives. J Am Chem Soc 135:7933–7937
Wooster TJ, Augustin MA (2006) β-Lactoglobulin-dextran Maillard conjugates: their effect on interfacial thickness and emulsion stability. J Colloid Interface Sci 303:564–572
Wüstneck R, Moser B, Muschiolik G (1999) Interfacial dilational behaviour of adsorbed β-lactoglobulin layers at the different fluid interfaces. Colloids Surf B: Biointerfaces 15:263–273
Wychowaniec JK, Patel R, Leach J, Mathomes R, Chhabria V, Patil-Sen Y, Hidalgo-Bastida A, Forbes RT, Hayes JM, Elsawy MA (2020) Aromatic stacking facilitated self-assembly of ultrashort ionic complementary peptide sequence: β-sheet nanofibres with remarkable gelation and interfacial properties. Biomacromolecules 21:2670
Yang Z, Gu H, Fu D, Gao P, Lam JK, Xu B (2004) Enzymatic formation of supramolecular hydrogels, Adv Mater 16:1440–1444
Yang X, Wang Y, Qi W, Su R, He Z (2017) Bioorganometallic ferrocene-tripeptide nanoemulsions. Nanoscale 9:15323–15331
Yang L, Qin X, Kan J, Liu X, Zhong J (2019) Improving the physical and oxidative stability of emulsions using mixed emulsifiers: casein-octenyl succinic anhydride modified starch combinations. Nano 9:1018

Ye A (2010) Surface protein composition and concentration of whey protein isolate-stabilized oil-in-water emulsions: effect of heat treatment. Colloids Surf B: Biointerfaces 78:24–29

Ye A, Singh H (2006) Adsorption behaviour of lactoferrin in oil-in-water emulsions as influenced by interactions with β-lactoglobulin. J Colloid Interface Sci 295:249–254

Ye A, Singh H (2007) Formation of multilayers at the interface of oil-in-water emulsion via interactions between lactoferrin and β-lactoglobulin. Food Biophys 2:125–132

Yildiz G, Ding J, Andrade J, Engeseth NJ, Feng H (2018) Effect of plant protein-polysaccharide complexes produced by mano-thermo-sonication and pH-shifting on the structure and stability of oil-in-water emulsions. Innovative Food Sci Emerg Technol 47:317–325

Zarai Z, Balti R, Sila A, Ali YB, Gargouri Y (2016) Helix aspersa gelatin as an emulsifier and emulsion stabilizer: functional properties and effects on pancreatic lipolysis. Food Funct 7:326–336

Zhai J, Wooster TJ, Hoffmann SV, Lee T, Augustin MA, Aguilar M (2011) Structural rearrangement of β-lactoglobulin at different oil–water interfaces and its effect on emulsion stability. Langmuir 27:9227–9236

Zhang S, Lockshin C, Cook R, Rich A (1994) Unusually stable β-sheet formation in an ionic self-complementary oligopeptide, biopolymers. Original Res Biomol 34:663–672

Zhang Y, Tan C, Abbas S, Eric K, Zhang X, Xia S, Jia C (2014) The effect of soy protein structural modification on emulsion properties and oxidative stability of fish oil microcapsules. Colloids Surf B: Biointerfaces 120:63–70

Zhang Y, Tan C, Abbas S, Eric K, Xia S, Zhang X (2015) Modified SPI improves the emulsion properties and oxidative stability of fish oil microcapsules. Food Hydrocoll 51:108–117

Zhao C, Dwyer MD, Yu L, Middelberg AP (2017) From folding to function: design of a new switchable biosurfactant protein. ChemPhysChem 18:488–492

Zhu Y, Chen X, McClements DJ, Zou L, Liu W (2018) pH-, ion- and temperature-dependent emulsion gels: fabricated by addition of whey protein to gliadin-nanoparticle coated lipid droplets. Food Hydrocoll 77:870–878